

The Shear Strength of Rock Joints in Theory and Practice

By

N. Barton and V. Choubey

With 20 Figures

(Received October 4, 1976)

Summary — Zusammenfassung — Résumé

The Shear Strength of Rock Joints in Theory and Practice. The paper describes an empirical law of friction for rock joints which can be used both for extrapolating and predicting shear strength data. The equation is based on three index parameters; the joint roughness coefficient *JRC*, the joint wall compressive strength *JCS*, and the residual friction angle ϕ_r . All these index values can be measured in the laboratory. They can also be measured in the field. Index tests and subsequent shear box tests on more than 100 joint samples have demonstrated that ϕ_r can be estimated to within $\pm 1^\circ$ for any one of the eight rock types investigated. The mean value of the peak shear strength angle ($\arctan \tau/\sigma_n$) for the same 100 joints was estimated to within $1/2^\circ$. The exceptionally close prediction of peak strength is made possible by performing self-weight (low stress) sliding tests on blocks with throughgoing joints. The total friction angle ($\arctan \tau/\sigma_n$) at which sliding occurs provides an estimate of the joint roughness coefficient *JRC*. The latter is constant over a range of effective normal stress of at least four orders of magnitude. However, it is found that both *JRC* and *JCS* reduce with increasing joint length. Increasing the length of joint therefore reduces not only the peak shear strength, but also the peak dilation angle and the peak shear stiffness. These important scale effects can be predicted at a fraction of the cost of performing large scale in situ direct shear tests.

Key Words: shear strength, joint, shear test, friction, compressive strength, weathering, roughness, dilation, stiffness, scale effect, prediction.

Die Scherfestigkeit von Kluftflächen in Theorie und Praxis. Zur Ermittlung der Reibungswerte in Kluftflächen wird ein empirisches Gesetz beschrieben, das sowohl das Extrapolieren als auch das Voraussagen von Scherfestigkeitszahlen ermöglicht.

Die Gleichung ist auf drei Indexzahlen gegründet: Den Rauigkeitskoeffizienten der Kluft *JRC* (Joint Roughness Coeff.), die Druckfestigkeit des Felses der Kluftwände *JCS* (Joint Wall Compression Strength) und der residuelle Reibungswinkel der Trennfläche ϕ_r .

Die Indexzahlen können alle im Laboratorium bestimmt oder am Ort gemessen werden. Bestimmung von Indexzahlen mit nachfolgender Prüfungen im Scherapparat von mehr als 100 Kluftproben haben erwiesen, daß für jede beliebige der acht untersuchten Gesteinsarten der Reibungswinkel ϕ_r auf $\pm 1^\circ$ genau geschätzt werden kann.

Der Durchschnittswert des Reibungswinkels ($\arctan(\tau/\sigma_n)$) der Höchstscherfestigkeit wurde für dieselben 100 Klüfte auf $\pm 1/2^\circ$ genau geschätzt. Die besonders genaue Vorausschätzung der Höchstscherfestigkeit ist durch Eigengewicht-Gleitversuche (niedrige Spannungen) auf Gesteinsblöcken mit durchgehenden Trennflächen ermöglicht. Der totale Reibungswinkel ($\arctan \tau/\sigma_n$), bei dem das Gleiten eintritt, ergibt eine Abschätzung des Rauigkeitskoeffizienten der Kluft JRC . Der Rauigkeitskoeffizient bleibt über einen Normal-Spannungsbereich von mindestens vier Größenanordnungen konstant. Die Indexzahlen JRC (Rauigkeitskoeffizient) und JCS (Druckfestigkeitskoeffizient) reduzieren sich aber bei zunehmenden Kluftlängen. Bei zunehmender Kluftflächengröße nehmen nicht nur die Höchstscherfestigkeit, sondern auch der zugehörige Dilatanzwinkel und die Schubsteifigkeit ab. Diese wichtigen Einflüsse der geometrischen Abmessungen können geschätzt und zahlenmäßig erfaßt werden, und zwar mit Kosten, die nur einen Bruchteil von denen betragen, die für große, direkte Scherversuche in situ erforderlich wären.

Schlüsselwörter: Scherfestigkeit, Trennflächen, Schertest, Reibung, Druckfestigkeit, Verwitterung, Rauigkeit, Dehnung, Steifigkeit, Einfluß der Abmessungen, Vorhersage.

La résistance au cisaillement des joints de roches en théorie et en pratique. Le rapport traite d'une loi empirique du frottement dans les joints de roches, loi pouvant être utilisée tant pour l'extrapolation que pour la prédiction de données relatives à la résistance au cisaillement. L'équation est basée sur trois indices de paramètres: coefficient de rugosité du joint (joint roughness coefficient — JRC), résistance de la paroi à la compression (joint wall compressive strength — JCS), et l'angle de frottement résiduel ϕ_r . Toutes ces valeurs d'indice peuvent être mesurées au laboratoire. Elles peuvent aussi l'être in situ. Des tests d'indice, avec ensuite des tests en boîte de cisaillement, sur plus de 100 échantillons de joints, ont permis de constater que, pour n'importe quel des huit types de roche étudiés, l'angle de frottement ϕ_r peut être évalué avec une précision de $\pm 1^\circ$. La valeur moyenne de l'angle maximum de la résistance au cisaillement ($\arctan \tau/\sigma_n$) pour les mêmes 100 joints fut évaluée avec une précision de $1/2^\circ$. La prédiction particulièrement précise de la résistance maximum au cisaillement est rendue possible par la réalisation d'essais de glissement dits "de poids propre" (faible contrainte) sur des blocs à joints passant de part en part. L'angle de frottement total ($\arctan \tau/\sigma_n$) auquel le glissement se manifeste, fournit une estimation du coefficient de rugosité du joint, JRC . Ce dernier est constant à l'intérieur d'une plage de tensions normales effectives d'au moins quatre ordres de grandeur. Cependant, on a trouvé que les indices JRC (rugosité) comme ceux JCS (compression) diminuent quand la longueur du joint augmente. Ainsi, si la longueur du joint augmente, cela réduira non seulement la résistance maximum au cisaillement, mais aussi l'angle maximum de dilatation et la rigidité maximum de cisaillement. Ces importants effets d'échelle peuvent être prédits, et ce à des coûts ne représentant qu'une fraction de ceux liés à des tests directs de cisaillement effectués in situ.

Mots-clés: résistance au cisaillement, joint, essai de cisaillement, frottement, résistance à la compression, dilatation, rugosité, dilatation, rigidité, effet d'échelle, prédiction.

Introduction

The term rock joint is used to describe the mechanical discontinuities of geological origin, that intersect almost all near-surface rock masses. In this paper both weathered and unweathered joints will be considered.

However, filled joints containing soft plastic materials such as clay, and faults containing gouge or breccia will not be included, since they constitute a rather special set of problems. The exclusion of filled joints means that weathering and alteration will only be considered if the walls of a joint are in rock to rock contact. The mechanical difference between contacting and non-contacting joint walls will usually result in widely different shear strength and deformation characteristics. In the case of unfilled joints the *roughness* and *compressive strength* of the joint walls are all important, while in the case of filled joints the physical and mineralogical properties of the material *separating* the joint walls are of primary concern.

The most important external factor affecting shear strength is the magnitude of the effective normal stress (σ_n) acting across the joint. In many rock engineering problems the maximum effective normal stress will lie in the range 0.1 to 2.0 MN/m² (1 to 20 kg/cm²) for those joints considered critical for stability. This is about three orders of magnitude lower than that used by tectonophysicists, when studying the shear strength of laboratory induced faults, under stress levels of for example 100 to 2000 MN/m² (1 to 20 kilobars). In consequence, the literature contains shear strength data for rock joints spanning a stress range of at least four orders of magnitude. It is partly for this reason that opinions concerning shear strength vary so widely.

It has been customary to fit Coulomb's linear relation.

$$\tau = c + \sigma_n \tan \phi \quad (1)$$

to the results of shear strength investigations on rock joints. (τ =peak shear strength, c =cohesion intercept, ϕ =friction angle). If this equation is applied to the results of shear tests on *rough joints*, under both high normal stress and low normal stress, one finds the tectonophysicist recording a cohesion intercept of tens of MN/m² and a friction angle of perhaps only 20°, while the rock slope engineer finds that he has a friction angle of perhaps 70° and zero cohesion. The peak shear strength envelopes for *non-planar* rock joints are in fact strongly curved.

This fact was recognised by Jaeger (1959), Krsmanović and Langof (1964), Lane and Heck (1964), Patton (1966) and Byerlee (1967), and by increasing numbers of investigators during the past ten years. However, the habit remains of describing the shear strength in terms of Coulomb's "constants" c and ϕ . Both are in fact stress dependent variables. They are also scale dependent.

Contact Area and Contact Stress

Before introducing a more satisfactory method of describing the shear strength of rock joints it is worth examining the need for empiricism. Stability calculations both in soil and rock mechanics are carried out in terms of "conventional" stress. That is to say, a given stress level is equal to (effective) force divided by gross area, with no consideration for the atomic, microscopic or visible contact area. Yet it is known that the contact area

involved when shearing rock joints is extremely small, as shown for example by Jaeger (1971) and Barton (1971a). According to the damage visible at the end of a shear test, the real contact area may be anything from one tenth to one thousandth (or less) of the gross area. The present series of shear tests on rocks with *joint wall compressive strengths* (*JCS* values) ranging from about 20 to 200 MN/m² in fact suggest that the contact area ratio (gross/real) may be closely related to the ratio JCS/σ_n applied in a given test. In a typical rock mechanics design problem with $JCS=100$ MN/m² and $\sigma_n=0.1$ MN/m² the real shear and normal stresses acting across the asperities visibly in contact may perhaps be as much as a thousand times higher than the conventional stresses. It is therefore not surprising that an empirical formulation is required to correctly describe shear strength, when conventional stress terms are used.

Empirical Equation of Shear Strength

The empirical relationship to be described here is unusual in that it can be used both to fit or extrapolate experimental data and even to *predict* it. The three constants involved can be determined so accurately from simple index tests that it has been possible to predict the *mean* peak shear strength angle ($\arctan \tau/\sigma_n$)⁰ of over 100 joint specimens to within 1/2⁰. These surprising experimental results are reported later in this paper.

The derivation of the empirical relationship was described by Barton (1973). It is written as follows:

$$\tau = \sigma_n \tan \left[JRC \log_{10} \left(\frac{JCS}{\sigma_n} \right) + \phi_b \right] \quad (2)$$

where τ = peak shear strength

σ_n = effective normal stress

JRC = joint roughness coefficient

JCS = joint wall compressive strength

ϕ_b = basic friction angle (obtained from residual shear tests on flat unweathered rock surfaces)

The families of peak strength envelopes shown in Fig. 1 illustrate the practical nature of this empirical law of friction. Values of JRC of 20, 10 and 5 are used to illustrate the effect of joint roughness, while the curve numbering 5, 10, 50, 100 (units of MN/m²) illustrate the effect of the joint wall compressive strength (JCS). (In passing it should be noted that the envelopes predicted for the roughest joints have been truncated to a curvi-linear form. $\arctan \tau/\sigma_n = 70^\circ$ is the suggested maximum allowable shear strength for design purposes). In Fig. 1 a basic friction angle of 30° has been assumed throughout. The value of ϕ_b for most smooth *unweathered* rock surfaces in fact lies between 25° and 35° , as can be seen from Table 1. It will be shown later that for the case of weathered joints, the residual friction angle ϕ_r ($< \phi_b$) can be substituted for ϕ_b in Eq. (2). Methods for estimating ϕ_r for weathered joints are described later.

Practical Application of Method

Eq. (2) can be used in three different ways:

- (i) Curve fitting to experimental peak shear strength data;
- (ii) extrapolation of experimental peak shear strength data;
- (iii) prediction of peak shear strength.

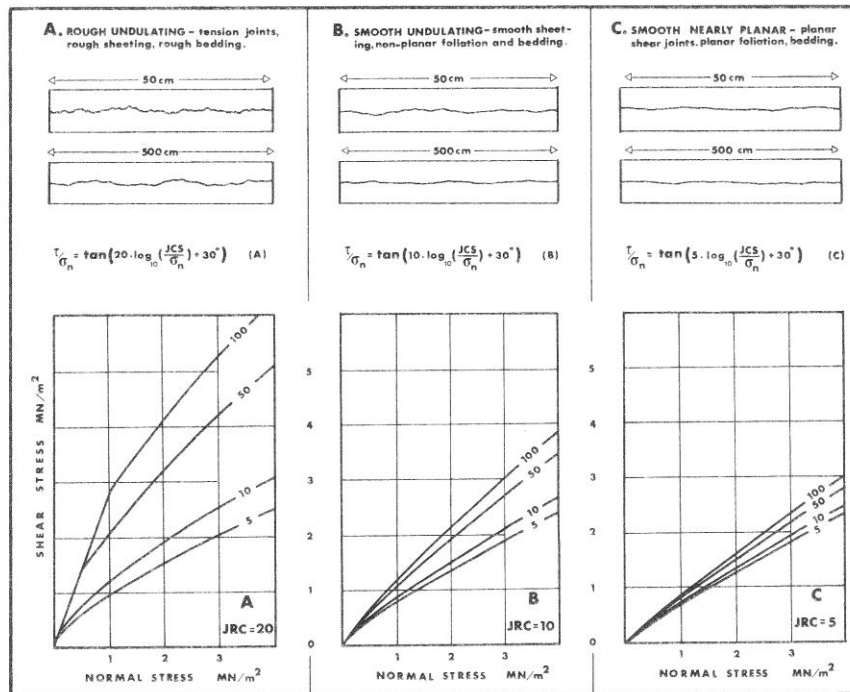


Fig. 1. Empirical law of friction in graphical form. Each curve is numbered with the appropriate JCS value (units of MN/m^2). The roughness profiles are intended as an approximate guide to the appropriate JRC values 20, 10 and 5. Completely smooth planar joints have $JRC = 0$

Zeichnerische Darstellung vom empirischen Gesetz für Reibung. Jede Kurve ist mit dem zutreffenden JCS -Wert (Einheit MN/m^2) numeriert. Die Rauigkeitsprofile geben eine Anleitung zur Schätzung der JRC -Werte 20, 10 und 5. Ganz glatte und ebene Klüfte haben $JRC = 0$

Loi empirique de frottement représentée graphiquement. Chaque courbe est numérotée à l'aide de la valeur JCS correspondante (nombres de MN/m^2). Les profils de rugosité donnent une indication pour l'appréciation approximative des valeurs JRC 20, 10 et 5. Les joints complètement lisses et planes ont une valeur $JRC = 0$

If one or more shear test have been performed, then the two variables in Eq. (2) (τ and σ_n) are known. The value of ϕ_b can normally be estimated with the help of the data listed in Table 1, unless the joints are strongly

Table 1. Basic Friction Angles of Various Unweathered Rocks Obtained From Flat and Residual Surfaces

Rock type	Moisture condition	Basic friction angle ϕ_b	Reference
A. Sedimentary Rocks			
Sandstone	Dry	26—35	Patton, 1966
Sandstone	Wet	25—33	Patton, 1966
Sandstone	Wet	29	Ripley & Lee, 1962
Sandstone	Dry	31—33	Krsmanović, 1967
Sandstone	Dry	32—34	Coulson, 1972
Sandstone	Wet	31—34	Coulson, 1972
Sandstone	Wet	33	Richards, 1975
Shale	Wet	27	Ripley & Lee, 1962
Siltstone	Wet	31	Ripley & Lee, 1962
Siltstone	Dry	31—33	Coulson, 1972
Siltstone	Wet	27—31	Coulson, 1972
Conglomerate	Dry	35	Krsmanović, 1967
Chalk	Wet	30	Hutchinson, 1972
Limestone	Dry	31—37	Coulson, 1972
Limestone	Wet	27—35	Coulson, 1972
B. Igneous Rocks			
Basalt	Dry	35—38	Coulson, 1972
Basalt	Wet	31—36	Coulson, 1972
Fine-grained granite	Dry	31—35	Coulson, 1972
Fine-grained granite	Wet	29—31	Coulson, 1972
Coarse-grained granite	Dry	31—35	Coulson, 1972
Coarse-grained granite	Wet	31—33	Coulson, 1972
Porphyry	Dry	31	Barton, 1971b
Porphyry	Wet	31	Barton, 1971b
Dolerite	Dry	36	Richards, 1975
Dolerite	Wet	32	Richards, 1975
C. Metamorphic Rocks			
Amphibolite	Dry	32	Wallace et al., 1970
Gneiss	Dry	26—29	Coulson, 1972
Gneiss	Wet	23—26	Coulson, 1972
Slate	Dry	25—30	Barton, 1971b
Slate	Dry	30	Richards, 1975
Slate	Wet	21	Richards, 1975

weathered. If the joints are completely unweathered then JCS will be equal to the unconfined compression strength of the unweathered rock (σ_c). The compression strength can be estimated quite well from point load tests on rock core or irregular lumps, as described by Broch and Franklin (1972). However, in general rock joint walls are weathered to some extent and JCS will be lower than σ_c . The relevant value is then measured using a Schmidt hammer applied directly to the exposed joint walls. The rebound value is converted to an estimate of compressive strength using Miller's (1965) method.

This type of index test is ideally suited, since the results are sensitive to the lower strength of the thin "skin" of weathered rock found along most joints. The method is fully described later.

The remaining unknown is the joint roughness coefficient JRC . This is estimated by back-analysing the shear tests that have been performed. Thus, rearranging Eq. (2):

$$JRC = \frac{\arctan(\tau/\sigma_n) - \phi_b}{\log_{10}(JCS/\sigma_n)} \quad (3)$$

To take an example, let us suppose that three shear tests have been performed and the following mean values have been estimated or measured as the case may be:

$$\begin{aligned} \text{peak } \arctan(\tau/\sigma_n) &= 50^\circ \\ \phi_b &= 30^\circ \\ JCS &= 100 \text{ MN/m}^2 \text{ (mean estimate from Schmidt rebound tests)} \\ \sigma_n &= 1 \text{ MN/m}^2 \text{ (mean value applied in the three shear tests)} \end{aligned}$$

According to Eq. (3) the mean JRC value is equal to 10. The task of *curve fitting* and *extrapolation* is now a simple matter. The relevant values of the three constants JCS , JRC and ϕ_b are simply substituted in Eq. (2) for the desired range of σ_n . It should be noted that if the above shear tests were performed with saturated joints then the index values of JCS and ϕ_b should also be based on wet surfaces, since JCS will usually be some 5 to 20% lower, and ϕ_b may also be lower in the case of saturated surfaces.

If the problem was one of *prediction* of peak shear strength, the same procedure is followed for estimating JCS and ϕ_b , but in this case JRC also has to be estimated. This can be done by crude visual comparison of roughness with the profiles given in Fig. 1, or with the more comprehensive set of roughness profiles reproduced later in this paper (Fig. 8).

However, the most satisfactory method is to estimate JRC by back-calculation, based on a remarkably simple index test. Blocks of rock intersected by the joint in question are removed from the rock face and are carefully tilted until the joint is so steeply inclined that the upper half of the block slides down the joint. The extremely low value of σ_n acting when sliding occurs is substituted in Eq. (3), together with the estimates of JCS and ϕ_b . In this instance the value of $\arctan(\tau/\sigma_n)$ is equal to the dip of the joint when sliding occurs since the shear stress τ and effective normal stress σ_n are both generated by the weight of the top half of the block. Alternatively this type of index test can be performed with the joint horizontal, the upper block being sheared by pushing or pulling horizontally, using for example a calibrated spring or hydraulic jack.

Summary of Experimental Results

The above tilt and push/pull tests undoubtedly sound rather crude. However, in the experimental study to be reported here, the mean results of tilt tests on 57 jointed specimens (joints smooth enough for this type of

test to be possible without the tilt angle approaching 90°) gave a mean estimated JRC value of 5.4, while the mean value back-calculated from the standard shear box tests on the same 57 joints was 5.5. It was therefore possible to predict the mean measured value of peak $\arctan(\tau/\sigma_n)^0$ to within 0.2° . (Mean measured value = 40.5° , mean predicted value = 40.3°). The push tests performed on 45 joints that were too rough for tilt testing did not give quite such impressive results, but the agreement would certainly be considered close enough for all practical purposes. (Mean predicted $JRC=9.9$, mean measured $JRC=9.3$. Mean predicted $\arctan(\tau/\sigma_n)=52.2^\circ$, mean measured $\arctan(\tau/\sigma_n)=50.9^\circ$).

Out of a total of 136 joint samples the remaining 34 had JRC values in excess of 12, which meant that the joints were too rough even for push tests to be performed. The only way of predicting JRC for these surfaces without performing shear tests under appreciable effective normal stress levels is to compare their surface roughness with joint surfaces that have already been tested (Fig. 8).

Joint Wall Compression Strength (JCS)

The measurement of this parameter is of fundamental importance in rock engineering since it is largely the thin layers of rock adjacent to joint walls that control the strength and deformation properties of the rock mass as a whole. Naturally the importance of the parameter is accentuated if the joint walls are weathered, since then the JCS value may be only a small fraction of the strength (σ_c) associated with the majority of the rock mass, as typically sampled by bore core.

The depth of penetration of weathering into joint walls presumably depends on rock type, in particular on its permeability. A permeable rock will tend to be weakened throughout, while impermeable rocks will just develop weakened joint walls, leaving relatively unweathered rock in the interior of each block. The weathering process of a rock mass can perhaps be summarized in the following simplified stages:

- 1) Formation of joint in intact rock; JCS value same as σ_c since no weathering.
- 2) Slow reduction of joint wall strength if joints are water-conducting; JCS becomes less than σ_c .
- 3) Common intermediate stage; weathered, water conducting joints, impermeable rock blocks between, JCS some fraction of σ_c .
- 4) Penetration of joint weathering effect into rock blocks; progressive reduction of σ_c from the walls of the blocks inwards, JCS continues to reduce slowly.
- 5) Advanced stage of weathering; more uniformly reduced σ_c finally drops to same level as JCS , rock mass permeable throughout.

The JCS values corresponding to stages 1 and 5 can be obtained by conventional unconfined compression tests on intact cylinders or from point

load tests on rock core or irregular lumps, though there might be sampling problems in the case of stage 5. Point load testing has been described in detail by Broch and Franklin (1972). In view of the fact that point load tests can be performed on core discs down to a few centimeters in thickness, it might also be possible to use this test for stage 4 on the core pieces on each side of deeply weathered joints. However, the JCS values relevant to stages 2 and 3 cannot be evaluated by these standard rock mechanics tests. The thickness of material controlling shear strength may be as little as a fraction of a millimeter (for planar joints) up to perhaps a few millimeters (for rough, weathered joints) with the limits depending on the ratio JCS/σ_n which basically controls the amount of asperity damage for a given joint roughness.

Schmidt Hammer Index Test

The Schmidt hammer provides the ideal solution to this dilemma. This is a simple device for recording the rebound of a spring loaded plunger after its impact with a surface. The L-hammer used here (impact energy = 0.075 mkg) is described by the manufactures as being "suitable for testing small and impact-sensitive parts of concrete or artificial stone". It is suitable for measuring JCS values down to about 20 MN/m² and up to at least 300 MN/m².

A wide ranging assessment of the suitability of the Schmidt hammer for use in rock mechanics was given by Miller (1965). He found a reasonable correlation between the rebound number (range 10 to 60) and the unconfined compression strength (σ_c) of the rock. However, a better correlation was obtained when he multiplied the rebound number by the dry density of the rock.

$$\log_{10} (\sigma_c) = 0.00088 \gamma R + 1.01 \quad (4)$$

where (σ_c) = unconfined compression strength of surface (MN/m²)

γ = dry density of rock (kN/m³)

R = rebound number

The above relationship and an approximate measure of the anticipated scatter is shown in Fig. 2. For present purposes the value of σ_c obtained for a given value of R and γ will represent the JCS value of the surface. For convenience the symbol (R) will be taken to represent the results of rebound tests on unweathered rock surfaces, while (r) will be used for tests on joint surfaces.

Some practical testing details need to be observed when using the Schmidt hammer.

1. Orientation

For a given surface the rebound number is minimum when the hammer is used vertically downwards (rebound against gravity) and maximum when used vertically upwards. Eq. (4) and Fig. 2 apply to vertical downwards tests on horizontal surfaces. The correlations given in Table 2 should be applied

when the hammer is used in other directions. The hammer should always be applied perpendicular to the surface in question.

2. Sample Dimensions

A correct rebound measurement will not be obtained if the impulse of the Schmidt hammer (from spring-fired projectile) is sufficient to move the rock sample being tested. Thus, if small samples such as rock core or

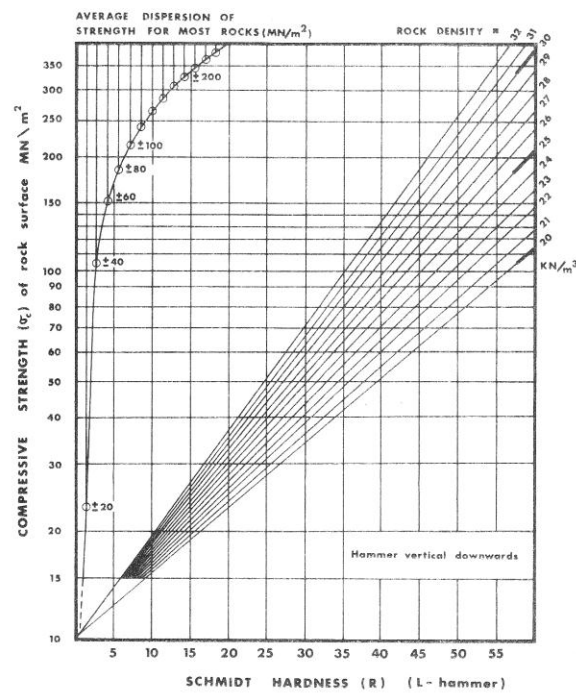


Fig. 2. Correlation chart for Schmidt (L) hammer, relating rock density, compressive strength and rebound number, after Miller (1965)

Korrelationskurven für Schmidt (L) Hammer zeigen Zusammenhang zwischen Felsdichte, Druckfestigkeit und Rückprallwerte nach Miller (1965)

Graphique de corrélation pour Schmidt (L) marteau. Indique le rapport entre densité de roche, résistance à la compression et valeurs de rebond, selon Miller (1965)

small blocks are to be tested, they should be firmly seated or clamped on a heavy base. Larger blocks extracted from rock slopes or tunnel walls

that are to be tested unclamped should, roughly speaking, measure at least 20 cm in each direction. A concrete (or rock) test floor and stable non-rocking blocks are advisable if blocks are no larger than this suggested minimum.

Table 2. Corrections for Reducing Measured Schmidt Hammer Rebound (R) When the Hammer Is Not Used Vertically Downwards (from Manufacturer's data)

Rebound R	Downwards		Upwards		Horizontal $\alpha = 0^\circ$
	$\alpha = -90^\circ$	$\alpha = -45^\circ$	$\alpha = +90^\circ$	$\alpha = +45^\circ$	
10	0	-0.8	—	—	-3.2
20	0	-0.9	-8.8	-6.9	-3.4
30	0	-0.8	-7.8	-6.2	-3.1
40	0	-0.7	-6.6	-5.3	-2.7
50	0	-0.6	-5.3	-4.3	-2.2
60	0	-0.4	-4.0	-3.3	-1.7

In the field, and the Schmidt hammer is essentially a field tool, such problems do not normally arise. However, if the rock mass is “drummy” for instance due to slabbing in a tunnel wall, artificially low rebound values may be obtained. A closely spaced and loose joint structure (i. e. phyllite) will also render results unreliable. It is normally possible to “hear” unreliable results during a set of tests, in just the same way that a geological hammer helps a geologist identify “drummy” rock. Sample extraction and clamping might be the only solution if heavily jointed rocks like phyllite are to be Schmidt hammer tested.

3. Number of Tests

Sample movement, “drumminess”, crushing of loose grains, etc., are some of the reasons for unexpectedly low rebound numbers in a given set of results. Unexpectedly high readings are seldom obtained. A convenient and realistic method of assessing the most relevant single value of (*r*) for a given joint surface is to take 10 readings (in different locations) on a representative sample or square meter, discount the five lowest readings, and take the mean of the five highest readings. Two typical sets of results taken from the present study are given below:

- a) rough, planar iron-stained joints in granite 44, 36, 38, 44, 32, 44, 44, 40, 34, 42
 mean of highest 5.....: *r*=44
 mean from 8 sets of readings...: *r*=43
 ($\gamma = 24.7 \text{ kN/m}^3$, hence mean
JCS = 88 MN/m², Fig. 2)
- b) rough, undulating calcite-coated joints in hornfels 28, 28, 30, 30, 28, 24, 24, 28, 30, 20
 mean of highest 5.....: *r* = 29
 mean from 3 sets of readings...: *r*=30
 ($\gamma = 30.1 \text{ kN/m}^3$, hence mean
JCS = 64 MN/m², Fig. 2)

4. Moisture

The reduction of compressive and tensile strength caused by increasing the moisture content of rock has been conclusively documented in the literature [see for instance Broch (1974) and Barton (1973)]. Generally a reduction of 10 to 30% can be expected from unconfined compression and point load tensile tests, between the crude engineering limits "air dry" and "saturated in situ".

The current study indicates that Schmidt hammer results for air dry and saturated joint surfaces also exhibit a significant reduction in strength. A variety of joint types in igneous and metamorphic rocks have shown average reductions in (*JCS*) values ranging between 5% and 18%, the largest reduction being for slate and gneiss and the smallest for granite. One very brittle fine grained hornfels indicated an increase of 9% for some unknown reason. On balance it would appear to be important to use the Schmidt hammer on wet joint surfaces, for the purpose of estimating minimum (*JCS*) values.

Estimation of Degree of Weathering or Alteration

The possible contrast in strength between the joint wall (represented by *JCS*) and the rock in the interior of the blocks (represented by σ_c) can serve as a useful indication of the character of joint weathering or alteration. Earlier studies (Barton, 1971b, 1973) indicated that the *relative alteration* (σ_c/JCS) can be as high as 4. In fact a *JCS* value equal to $1/4 \sigma_c$ probably represents a conservative lower bound if the *JCS* value has to be estimated in the absence of Schmidt hammer tests.

More recent work by Richards (1975) showed that a series of weathered joints in sandstone had values of *relative alteration* ranging from 1.8 to 3.8. In this case *JCS* values were obtained from Schmidt rebound tests on the weathered joint surfaces, while σ_c values were obtained from point load tests on rock adjacent to the particular joints. The samples were obtained from a quarry face which exhibited various degrees of weathering. If the various *JCS* values are compared with the point load tests on the freshest of all the sandstone samples ($\sigma_{c0} = 336 \text{ MN/m}^2$) it is found that the ratio σ_{c0}/JCS can be as high as 16. The intact rock weathered to one sixth of its unweathered strength ($\sigma_{c0}/\sigma_c = 6$).

In the present study values of *relative alteration* ranged from 5.2 to 1.0. The highest value was for calcite coated joints in a nodular hornfels, and the lowest value was for rough iron-stained joints in a permeable, coarse-grained, slightly altered granite. Most values lay between 1.4 and 1.9. All the values of σ_c were estimated from Schmidt rebound tests on saw-cut surfaces of rock adjacent to the joints. Saturated surfaces were used for estimation of both *JCS* and σ_c .

Variation of Rock Density With Weathering

Little appears to be known at present about either the density profile adjacent to a weathered joint wall, or the effect this may have on the inter-

pretation of JCS from Schmidt rebound tests (Fig. 2). An advanced stage of joint weathering or alteration would probably lead to locally reduced density, and presumably this should be allowed for when estimating JCS .

Richard's (1975) tests on sandstone joints indicated density reductions from approximately 25.5 to 23.5 kN/m³ from the unweathered to the most weathered sandstone. (JCS values ranged from approximately 114 to 21 MN/m², based on rebound values (r) of 46 down to 15). Martin and Millar (1974) reported a similar series of tests on joints in weathered sandstone. The maximum density of rock which gave joint rebound values (r) up to 40 was 25.7 kN/m³, while the next stage of weathering with (r) values down to 15 had a minimum density as low as 23.2 kN/m³. Thus far the results are closely comparable with those of Richards. However, the more severely weathered grades with (r) values in the range 0 to 20 had densities ranging all the way from 19.3 to 25.4 kN/m³.

In the present study attempts were initially made to saw off thin slices of joint wall material and compare the density obtained with that of rock more than 3 to 4 mm from the joint walls. Since the majority of the joints had values of *relative alteration* (σ_e/JCS) less than 2.0, it is perhaps not surprising that density variations were no more than 2%. In some cases the wall material was actually slightly denser, perhaps due to iron staining. Increases or reductions of this order are clearly of little significance when estimating JCS from Fig. 2, and they were ignored in these tests.

Table 3. Estimated Reductions in Density for Various Degrees of Relative Alteration

Relative alteration (σ_e/JCS)	% change in density (γ)
1—2	0%
2—3	—5%
3—4	—10%
4—10	—20%

In the absence of further data it may perhaps be worth following the crude guidelines set out in Table 3, if detailed studies of density variations are not carried out. The density reductions are roughly consistent with the results discussed above.

Basic Friction Angle (ϕ_b) and Residual Friction Angle (ϕ_r)

The comprehensive list of ϕ_b values listed in Table 1 are for the most part based on the residual strength exhibited by flat *unweathered* rock surfaces, which were most frequently prepared by diamond saw. In some cases these surfaces were sandblasted between tests. The friction angles obtained are clearly applicable to unweathered joint surfaces, and will not be applicable to weathered rock joints unless the level of effective normal stress applied is high enough for the thin layers of weathered rock to be worn away, thereby allowing contact between the fresher underlying rock (Richards, 1975).

Under low levels of effective normal stress the thin layers of weathered material, perhaps less than 1 mm in thickness, may continue to control the shear strength past peak strength and even for displacements up to residual strength. Richards' tests on weathered sandstone joints showed that it was possible to have residual friction angles (ϕ_r) for unfilled joints as low as 12° , if normal stress levels were low. His test results are reproduced in Fig. 3,

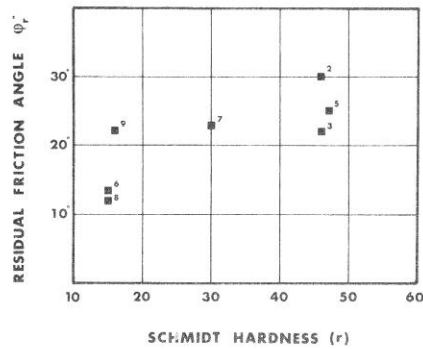


Fig. 3. Richards' (1975) results for seven weathered joints in sandstone, when tested at low normal stress (0.17 MN/m^2)

Die Ergebnisse für sieben verwitterte Klüfte in Sandstein unter kleinen Normalspannungen 0.17 MN/m^2 geprüft. Richards, 1975

Résultats de sept joints délités dans du grès, testés à de faibles tensions normales (0.17 MN/m^2). Richards (1975)

and indicate the strong correlation with the joint rebound value (r). Under high levels of normal stress the more resistant sandstone beneath the weathered skin came into effect and the mean value of ϕ_r obtained for the same seven specimens was 28.5° (range 19.5° to 33°).

An unpublished report of the above results (Richards, personal communication, 1974) stimulated the first author to look for a simple method of estimating ϕ_r from the results of Schmidt rebound tests. The first empirical relationship tried was as follows:

$$\phi_r = 10^\circ + r/R (\phi_b - 10^\circ) \quad (5)$$

where r = rebound on weathered joint surface

R = rebound on unweathered rock surface

This equation was later evaluated by Richards (1975), using a ϕ_b value of 30° which appears to be a realistic mean value for sandstone according to Table 1. Values of JRC equal to 5 or 10 were assigned to the seven sandstone joints by visual comparison with the profiles shown in Fig. 1. The measured joint rebound (r) for each specimen was converted to

the JCS value using Fig. 2, and with ϕ_r estimated from Eq. (5), it was possible to estimate the overall mean value of peak $\arctan(\tau/\sigma_n)$ for the seven joints to within 1° . (Measured mean = 38.6° , estimated mean = 37.6°). It was clear that for the general case of weathered and unweathered joints Eq. (2) should be written as follows:

$$\tau = \sigma_n \tan \left[JRC \log_{10} \left(\frac{JCS}{\sigma_n} \right) + \phi_r \right] \quad (6)$$

In the present work eight different rock types were studied, represented by 136 individual jointed specimens. The specimens were sawn from larger blocks containing throughgoing joints, which were extracted from road cuttings and quarries in the Oslo area. Since the object of the study was to develop simple methods for *estimating* peak shear strength, it made no sense having to measure ϕ_r for each specimen. Conversely, it was impractical to use Eq. (5) to estimate ϕ_r if the relevant value of ϕ_b could not be found in the literature (Table 1). A very simple solution was devised.

Residual Tilt Tests

The blocks of rock from which jointed specimens were sawn were retained. After thorough washing to remove the rock saw dust, and after air drying, pairs of flat sawn surfaces were mated, and the pairs of blocks tilted until sliding just occurred. As many as ten pairs of blocks were used to characterize each rock type.

The *residual tilt* test is basically a shear test under very low normal stress. In the present series of tests, block "overburden" depths ranged from 5 to 20 cm, and with most surfaces sliding when at a tilt angle of about 30° , the range of σ_n was approximately 1 to 5 kN/m² (0.01 to 0.05 kg/cm²). Following the tilt tests the same dry sawn surfaces were tested with the Schmidt hammer to obtain (R). The mean results obtained for seven of the eight types are shown in Fig. 4.

In the case of slate, the blocks from which samples were sawn disintegrated, due to the extreme friability of this cleaved rock. Schmidt hammer tests and residual tilt tests could not therefore be performed on the sawn surfaces of large blocks, as with the other seven rock types. (In this case ϕ_r was measured directly in a shear box, and averaged 26° .)

The empirical relation used here to estimate ϕ_r from the ϕ_b values obtained from residual tilt tests differs slightly from Eq. (5). The equation given below is preferred since it allows for a range of ϕ_r values even when the joint is very weathered. Eq. (5) tends to discount mineralogical differences since ϕ_r tends to a single minimum value of 10° when (r) is zero. The preferred relation is as follows:

$$\phi_r = (\phi_b - 20^\circ) + 20 (r/R) \quad (7)$$

where ϕ_b = basic friction angle estimated from residual tilt tests on *dry* unweathered sawn surfaces (or from Table 1)

R = Schmidt rebound on *dry* unweathered sawn surfaces

r = Schmidt rebound on *wet* joint surfaces

When Eq. (7) is used to estimate the relevant values of ϕ_r from the seven values of ϕ_b given in Fig. 4, the values given in Fig. 5 are obtained. These ϕ_r values are relevant to *saturated* conditions.

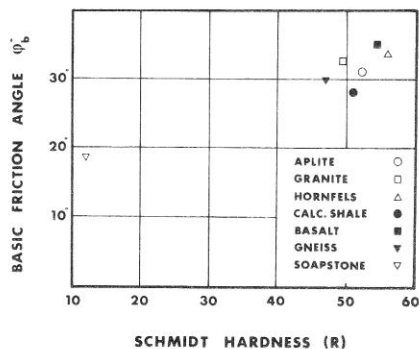


Fig. 4. Mean results of residual tilt tests to determine ϕ_b for unweathered rock. Both the tilt tests and the Schmidt rebound tests were performed on dry rock surfaces

Durchschnittliche Ergebnisse von Kippversuchen für Bestimmung des residuellen Reibungswinkels ϕ_b für unverwitterten Felsen. Die Kippversuche sowie die Schmidthammer-Proben wurden auf trockenen Klüftwänden gemacht

Résultats moyens obtenus aux essais de basculement destinés à déterminer l'angle ϕ_b pour roche non délitée. Les tests de basculement, comme ceux de rebondissement Schmidt, furent effectués sur des surfaces de roches sèches

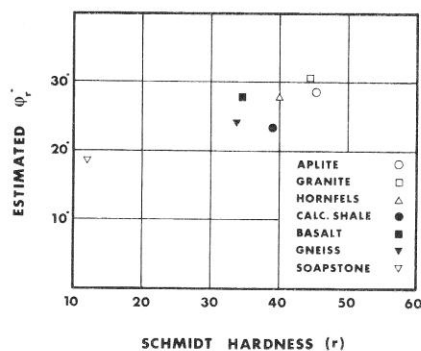


Fig. 5. Estimated values of ϕ_r obtained from Eq. (7) using the data in Fig. 4. The values are relevant to saturated surfaces

Reibungswerte ϕ_r errechnet aus Gl. (7) mit den Daten in Fig. 4. Die Werte beziehen sich auf gesättigte Oberflächen

Valeurs estimées de ϕ_r obtenues à partir de l'équation (7) à l'aide des données de la fig. 4. Les valeurs se rapportent à des surfaces saturées

For the benefit of those who are inherently and justifiably suspicious of empirical methods it should be pointed out that the ϕ_r values represented in Fig. 5, which ranged from 19° to 31° , were the values used in the shear strength prediction exercise summarized earlier. The fact that the *mean* peak shear strength angle of over 100 joint specimens can be estimated to within $1/2^\circ$ based on Eqs. (6) and (7) suggests that these empirical relationships reflect

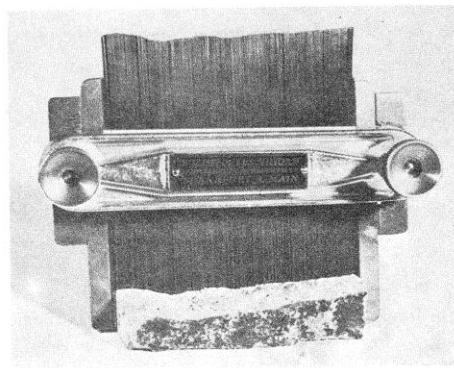


Fig. 6. Recording the roughness profiles for the joint surfaces before shear testing
Messen von Rauheitsprofilen der Klüftflächen vor der Scherprüfung
Mesurage des profils de rugosité des surfaces du joint avant l'essai de cisaillement

joint behaviour quite accurately. In fact it can be seen from Table 11 in the Appendix that individual errors in estimating ϕ_r for 15 different joint types were in no case more than -1.0° to $+0.8^\circ$ from the correct value. The error in estimating the *mean* ϕ_r value for over 100 joint specimens was only 0.1° .

Joint Roughness Coefficient (JRC)

In the preliminary stages of a rock engineering project it is helpful to be able to make a quick estimate to discover if the shear strength of the joints is so low that closer investigation is required. For example, ϕ_r could be estimated conservatively as 20° , σ_c could be estimated from experience and JCS approximated to $1/4 \sigma_c$. The only remaining estimate required is JRC .

Matching of Roughness Profiles

The crude estimates of JRC (5, 10 and 20) given by Barton (1973) and reproduced in Fig. 1 were designed as a preliminary guide for those unable to investigate the parameter JRC more closely. For this same pur-

Table 4. Description of Rock Joints Shown in Fig. 7

Sample no.	Rock type	Description of joint	JRC (back-calculated)
1	Slate	smooth, planar: cleavage joints, iron stained	0.4
2	Aplite	smooth, planar: tectonic joints, unweathered	2.8
3	Gneiss (muscovite)	undulating, planar: foliation joints, unweathered	5.8
4	Granite	rough, planar: tectonic joints, slightly weathered	6.7
5	Granite	rough, planar: tectonic joints, slightly weathered	9.5
6	Hornfels (nodular)	rough, undulating: bedding joints, calcite coatings	10.8
7	Aplite	rough, undulating: tectonic joints, slightly weathered	12.8
8	Aplite	rough, undulating: relief joints, partly oxidized	14.5
9	Hornfels (nodular)	rough, irregular: bedding joints, calcite coatings	16.7
10	Soapstone	rough, irregular: artificial tension fractures, fresh surfaces	18.7

pose, all the 136 joint specimens tested in the present study were profiled as shown in Fig. 6. In most cases, three profiles were measured on each

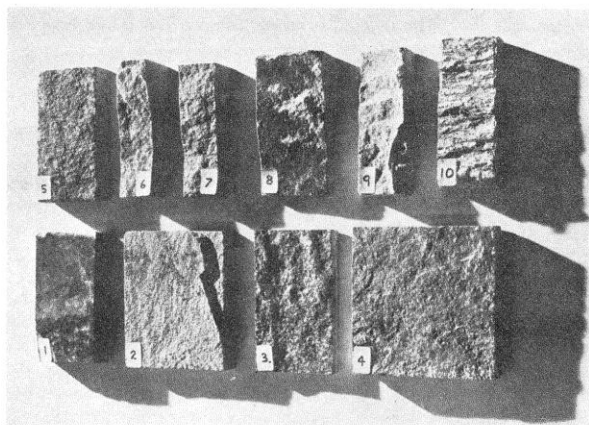


Fig. 7. Examples of the range of joint roughness studied. Corresponding profiles are given in Fig. 8

Beispiele von dem Variationsbereich der Rauigkeit der untersuchten Kluftproben
Exemples de la dispersion des rugosités de joints étudiées. Les profils correspondants sont reproduits sur la fig. 8

specimen. The *JRC* values back calculated from each share box test were grouped in the following ranges 0—2, 2—4 etc. up to 18—20. An attempt

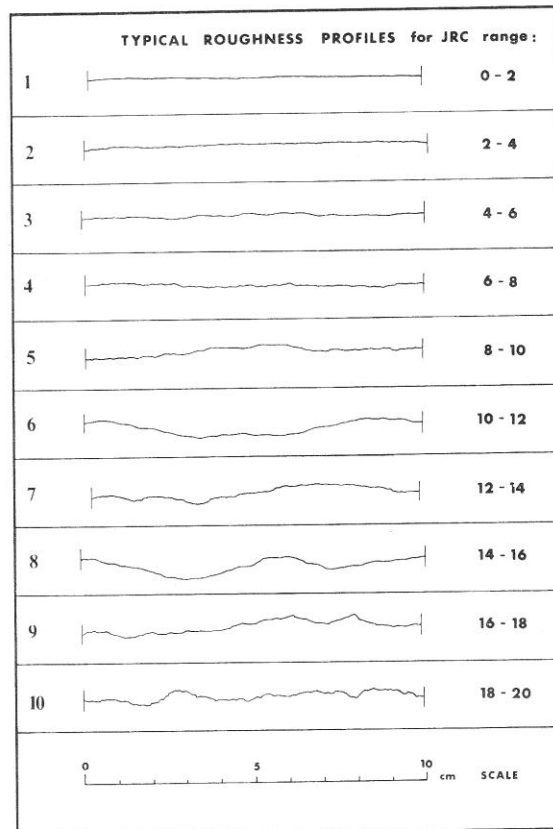


Fig. 8. Roughness profiles corresponding to the joints shown in Fig. 7, showing the typical range of *JRC* values associated with each one

Rauhigkeitsprofile für die Klüftflächen in Fig. 7 zeigen typische Geltungsbereiche der zugehörigen *JRC*-Werte

Les profils de rugosité des surfaces de joints de la fig. 7 montrent les zones de validité typiques des valeurs *JRC* correspondantes

was then made to select the most typical profiles of each group. It should be noted that in all cases where the mean joint plane was not within

$\pm 1^0$ of horizontal when placed in the shear box, the shear strengths and corresponding *JRC* values were corrected to the horizontal plane.

The particular joints chosen to represent specific *JRC* values are shown in Fig. 7, and the relevant profiles are reproduced in Fig. 8. Table 4 gives a description of the 10 surfaces. The verbal description of roughness, i. e. "undulating planar" refers to small scale and intermediate scale features, in that order.

In Situ Appearance of Selected JRC Values

Thirty eight of the joint samples were extracted from road cuttings through a coarse grained granite (Drammen granite), as illustrated in Fig. 9. A fine grained intrusive (aplite) from the same location yielded another

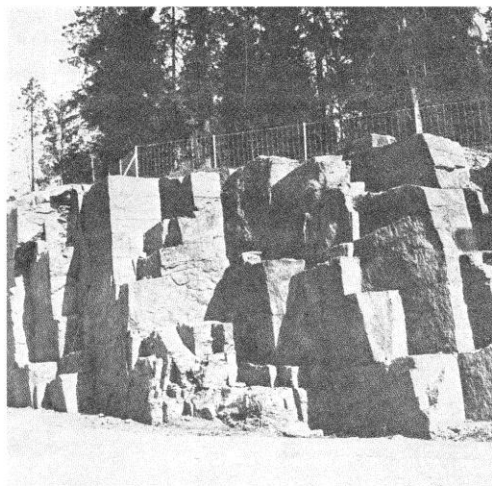


Fig. 9. In situ location typical for samples 4 and 5 (Table 4). The rock is coarse-grained Drammen granite located 25 km west of Oslo
 Feldaufnahme typisch für die Proben 4 und 5 (Tafel 4). Der Fels ist grob-körnig Drammen Granit, 25 km westlich von Oslo gelegen
 Situation typique in situ des échantillons 4 et 5 (Tableau 4). La roche est un granite à gros grain de la région de Drammen, à 25 km à l'ouest d'Oslo

thirty six joint samples. These two rock types are represented by Nos. 4 and 5 (granite) and 7 and 8 (aplite) in Fig. 7 and Table 4.

The purpose of Fig. 9 is to illustrate the *in situ* appearance of joints which, with sample lengths of 10 cm, yield *JRC* values typical of samples 4 and 5. The particular *JRC* values of 6.7 and 9.5 are quite typical of the vertical joints exposed in the sunlight in Fig. 9. The vertical joint set in the

shade has a roughness typified by sample 7 ($JRC=12.8$) while the roughness of sample 8 ($JRC=14.5$) is quite representative of the sub-horizontal relief joints seen in Fig. 9.

A very important factor which will be dealt with under the section on scale effects, is that the JRC value may be lower if larger joint samples are tested. Since there may also be a scale effect on JCS (as there is known to be for σ_c), the relevance of small scale laboratory tests to in situ conditions is questionable to say the least. (See Pratt, Black and Brace 1974 and Barton 1976b). The strength of the present empirical methods is that these scale effects can be incorporated in the estimate of shear strength in a realistic, consistent manner. This is more reliable than applying factors of safety (or ignorance) to (c) the cohesion and (ϕ) the friction angle, as sometimes done in design.

Estimation of JRC From Tilt Tests

The *residual tilt test* described earlier for measuring the basic friction angle ϕ_b for smooth unweathered rock surfaces is basically a test of the mineralogical properties of the rocks concerned. Although microscopic examination would undoubtedly show steep asperities ploughing into one another, on a *visible* scale the test has no roughness component. For all intents and purposes the surfaces are non-dilatant.

If the same type of tilt test is performed on a rough joint as illustrated in Fig. 10, the angle (α) at which sliding occurs may be 40° or 50° more than ϕ_b (and even higher compared to ϕ_r). This additional shear strength is due to the geometrical effect of roughness. The maximum dilation angle (d_0) when sliding occurs is probably given by the following simple relationship:

$$d_0 = \alpha - \phi_r \quad (8)$$

The tilt angle (α) is a function of the ratio between the shear stress (τ_0) and normal stress (σ_{n0}) acting on the joint when sliding occurs under these very low stress levels:

$$\alpha = \arctan (\tau_0 / \sigma_{n0}) \quad (9)$$

The effective normal stress (σ_{n0}) generated by the gravitational force acting on the upper half of the block is as follows for the case of an infinitely long block:

$$\sigma_{n0} = \gamma h \cos \alpha \quad (10)$$

where h = thickness of top half of block (m)
 γ = rock density (kN/m^3)

In the example illustrated in Fig. 10, where $h=0.025$ m, and $\gamma=25$ kN/m^3 , the value of σ_{n0} is theoretically equal to 0.22 kN/m^2 (0.0022 kg/cm^2) if the limited length/thickness ratio (approx. 4) is ignored. This is clearly an extremely low stress, being equivalent to an "overburden" of about 0.8 millimetres of rock.

In the present study the majority of joint samples had a length of 98 mm and the upper half of each pair of mating blocks averaged 23 mm in thickness. Based on these average dimensions it can be shown that the vertical line of action from the centre of gravity of the top block passes just outside the toe when the joint is inclined at 77° . The line of action passes outside the "central third" of the joint when the joint is inclined at 55° .

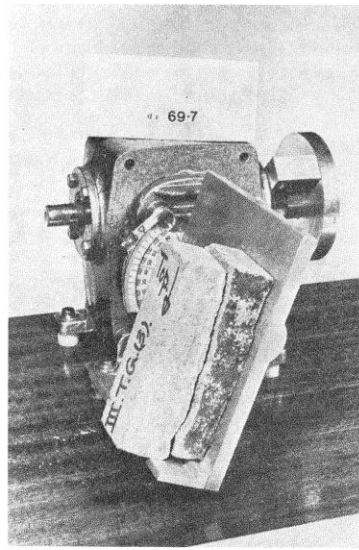


Fig. 10. Tilt test to determine the joint roughness coefficient (*JRC*) of a surface. The top half of the jointed sample slid when the joint was dipping at 69.7° .

Kippversuch zur Bestimmung des Rauigkeitskoeffizienten einer Kluffläche. Die obere Hälfte der geklüfteten Probe ist bei einem Neigungswinkel der Kluffläche von 69.7° abgerutscht.

Essai de basculement destiné à déterminer le coefficient de rugosité (*JRC*) d'une surface de joint. La moitié supérieure de l'échantillon à joint glissa au moment où l'angle d'inclinaison atteignit 69.7° .

The tendency for tension to be developed at the top of the joint plane, followed by actual overturning when the joint is even more steeply inclined, makes the theoretical stress distribution [Eq. (10)] for an infinite plane of questionable value. In addition the present length/thickness ratio of about 4 is probably more favourable than that to be expected in the field when two mating blocks are tilted during a larger scale version of these laboratory tests.

For the above reasons the following empirical relation has been used:

$$\sigma_{n0} = \gamma b \cos^2 \alpha \tag{11}$$

This makes some allowance for the uneven stress distribution, particularly when α is large. More important perhaps is that it automatically limits the

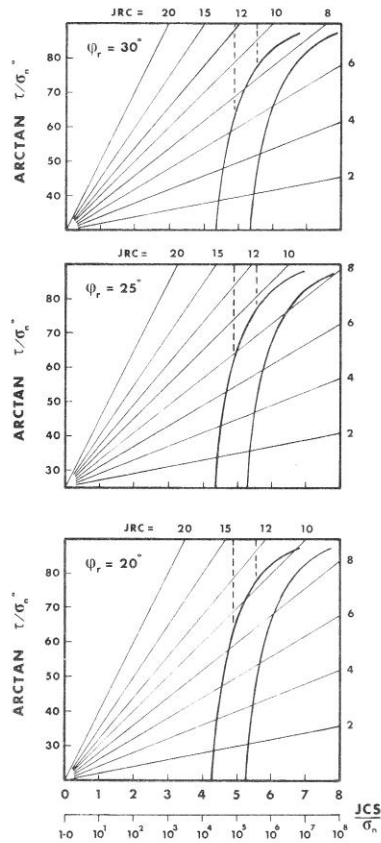


Fig. 11. Range of application of tilt tests and push/pull tests for determining *JRC* values of joints

Bereich der Verwendung von Kippversuchen und geschobenen/gezogenen Proben für die Bestimmung von *JCR*-Werten für Klufflächen

Zone d'application d'essais de basculement et d'essais de poussée/traction en vue de la détermination des valeurs *JRC* de joints

range of application of the tilt test to surfaces smooth enough to be tested without encountering overturning failure in place of sliding. The limits of application are illustrated in Fig. 11.

The 57 samples with joints smooth enough to be tilt tested, provided estimates of JRC that were accurate enough for the mean shear strength angle ($\arctan \tau/\sigma_n$) of the same samples to be predicted to within 0.2° . The empirical correction factor ($\cos \alpha$) used in Eq. (11) is therefore presumably realistic.

The JRC value is estimated from tilt tests using Eq. (6), by substituting the values of α and σ_{n0} . Thus:

$$JRC = \frac{\alpha - \phi_r}{\log_{10} \left(\frac{JCS}{\sigma_{n0}} \right)} \quad (12)$$

(Note that an underestimated ϕ_r value results in an overestimated JRC value, and vice versa. This automatic compensation of errors is one reason for the method providing such accurate estimates of peak $\arctan \tau/\sigma_n$.) The tilt test is performed on dry joints only, to avoid any possible problems with fluctuating joint water pressures, or capillarity. As such, the appropriate JCS value is that measured on the *dry* joints, using the Schmidt hammer as before. Three tilt tests are performed on each joint and the mean value is used for estimating JRC . Due to the very low stress level there is no visible damage, so the tilt test can be repeated many times without reduction in strength. For the example illustrated in Fig. 10, an undulating tectonic joint in aplite, the JRC value estimated from Eq. (11) and (12) was as follows:

$$JRC = \frac{69.7^\circ - 29^\circ}{\log_{10} (92/0.00075)} = \frac{40.7}{6.09} = 6.7$$

This JRC value, and the JCS value for the *saturated* joint (77 MN/m^2) can then be used to estimate the peak value of $\arctan (\tau/\sigma_n)$ of the *saturated* joint for any desired value of effective normal stress, using Eq. (6).

The problem of joint opening and overturning when a rough joint is steeply inclined means that the tilt test should not be attempted in the case of markedly rough joints. In Fig. 11, the empirical relationship expressed in Eq. (6) is represented in graphical form, for three realistic values of ϕ_r . The pairs of curved envelopes represent the approximate range of JRC values that can be reliably tested using the tilt method. The block thickness (b) assumed here ranges from 2 cm (laboratory sample, right hand curve) to 20 cm (field block, left hand curve), and JCS is assumed to be equal to 100 MN/m^2 . The curves were evaluated using Eq. (11), which incorporates a correction factor $\cos \alpha$, as discussed earlier. This factor, while changing the estimate of JRC very little, ensures that the tilt test is not used for joints rough enough to fail by overturning instead of sliding.

In the case of the present laboratory tests, the maximum value of JRC that could be obtained from the laboratory scale tilt tests was about 8 since the mean ϕ_r value for the 136 specimens was 27.5° . If field-scale tilt tests

were performed on strongly weathered joints ($\phi_r = 20^\circ$, Fig. 11) the limiting JRC value would be at least 10, especially if the JCS value was low due to the effects of weathering. In view of the fact that most stability problems are caused by the smoother joints, the above limitations of the tilt test will seldom be of importance.

Estimation of JRC From Push or Pull Tests

Rougher joints can be tested by means of "push" or "pull" tests, with the joint in a horizontal plane (or inclined as convenient) and the top block pushed or pulled parallel to the joint plane. In the present series of laboratory tests, each joint was first *dry tilt tested* (average of 3 tests), then placed in the direct shear box and *dry push tested* once, under the normal load generated by the weight of the top half of the specimen. The approximate range of application for this type of laboratory test is given by the stippled lines in Fig. 11. A maximum JRC value of about 12 could be tested satisfactorily in the present series of tests. In a field situation, with larger blocks and more weathered joints the range of JCS/σ_n might be as much as two orders of magnitude *lower*, thereby allowing joints as rough as $JRC=20$ to be tested in this way.

It is therefore possible to test the whole spectrum of joint roughness using a combination of tilt, push or pull tests. However, discontinuous joints and joints having vertical or very steep "steps" caused by cross jointing, display real cohesion and cannot generally be tested by such methods. This type of secondary jointing has such high shear strength that a stability problem will seldom arise if failure is limited to these surfaces. However, there are examples where failure has developed by "down-stepping" between two intersecting joint sets. In such cases it would be incorrect sampling practice to test joints with steps facing against the direction of shear. Tilt, push or pull tests (and eventual direct shear tests) should be conducted on the joint surfaces most likely to allow failure to initiate.

Comparison of Predicted and Measured Data

The results of the present series of tilt tests and push tests are given in Fig. 12. The tilt test data are relevant to all those joints (57) which had JRC values less than 8, according to back analysis of the conventional shear box tests on the same joints. The push test data are relevant to the joints (45) having JRC values in the range 8 to 12. The mean value of $\phi_r = 27.5^\circ$ used in plotting the sloping lines (where gradients equal JRC values) can only give an approximate picture of the real JRC values, since ϕ_r actually ranged from 23° to 31° for this set of 102 joints.

Despite the inevitable scatter of results, the *mean* values predicted and measured were very close. The *mean* value of JRC predicted from the tilt tests on the 57 smoothest joints was 5.4, while the measured *mean* obtained from back analysis of the conventional shear box tests was 5.5. The *mean* value of JRC predicted from the push tests on the 45 rougher joints was

9.9, while the measured *mean* was 9.3. If the 102 tests are combined the *mean* predicted *JRC* value is equal to 7.4, and the *mean* measured value 7.2.

One can conclude that *JRC* is essentially a constant for a given joint, since it does not appear to vary significantly even over a stress range of up to *five* orders of magnitude. Other studies by the first author (Barton, 1976b) have indicated that this extrapolation may also be performed for very rough

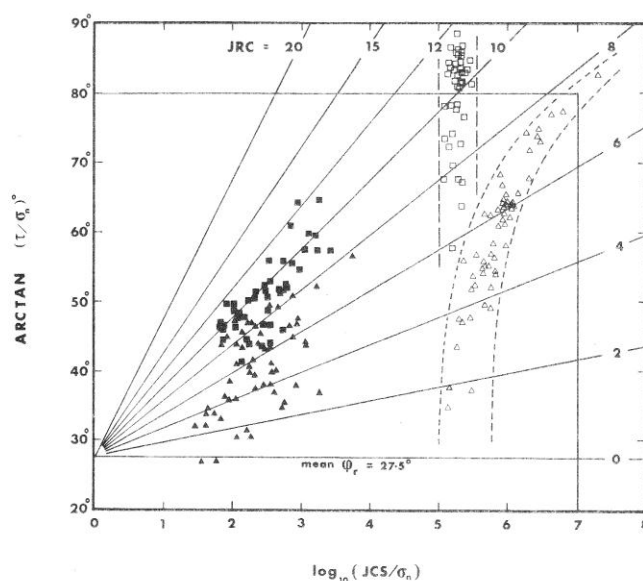


Fig. 12. The results of laboratory tilt tests (Δ) and push tests (\square), and the corresponding values of peak shear strength measured in the direct shear box using the same joints, under conventional levels of normal stress (approx. 0.05 to 1.5 MN/m²)

Die Resultate von Kippversuchen (Δ) und geschobenen Proben (\square) im Laboratorium und die zugehörigen in direkten Scherversuchen gemessenen Höchstschersfestigkeiten. Dieselben Klüffflächen wurden unter gebräuchlicher Normalspannung im Bereich 0.05 bis 1.5 MN/m² benutzt

Les résultats des essais de basculement (Δ) et des essais de poussée (\square) au laboratoire, et les valeurs maximum correspondantes de résistance au cisaillement mesurées dans l'appareil de cisaillement direct avec utilisation des mêmes joints, à des niveaux conventionnels de tension normale (env. 0,05 à 1,5 MN/m²)

joints, and over a stress range of up to *eight* orders of magnitude, spanning the whole brittle range of behaviour. This stress range can be visualized as an "overburden" of rock ranging from approximately 0.5 mm to 50 km.

The individual estimates of JRC obtained from each tilt or push test were used to predict the individual values of peak arctan (τ/σ_n) likely to be measured in the direct shear box under the conventional effective normal stress levels applied. A comparison of predicted and measured values is

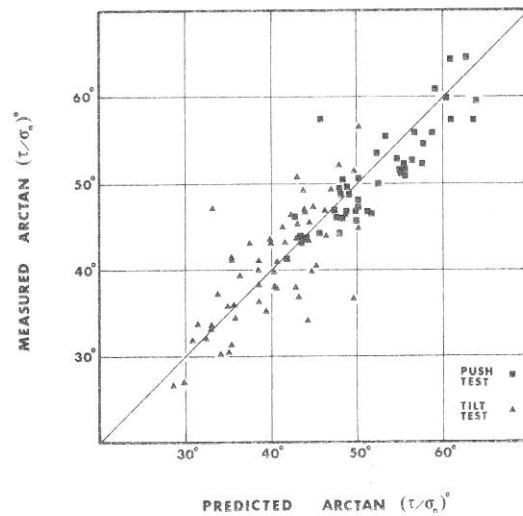


Fig. 13. Peak arctan (τ/σ_n) predicted from tilt and push tests compared with the measured values obtained from conventional shear box tests on the same joint samples

Durch Kipp- und Schub-Versuche vorausgesagte Höchstscherfestigkeiten ($\arctan \tau/\sigma_n$) verglichen mit den im direkten Scherversuch gemessenen Werten für dieselben Klüftproben
 Comparaison entre, d'une part, des valeurs maximales arctan (τ/σ_n) prédites sur la base d'essais de basculement et de poussée, et, d'autre part, des valeurs mesurées obtenues par des essais conventionnels en boîte de cisaillement, effectués sur les mêmes échantillons de joints

given in Fig. 13. The mean value of arctan (τ/σ_n) predicted from the 57 *tilt tests* was 40.3° , and the measured mean was 40.5° . In the case of the 45 *push tests* on the rougher joints, the predicted and measured means were 52.2° and 50.9° respectively. The overall means for the 102 specimens were 45.6° (predicted) and 45.1° (measured).

Summary of Prediction Errors for 15 Different Joint Types

The remarkably close *mean* values discussed above may leave the false impression that only *one* tilt or push test need be performed to characterize the shear strength of a whole joint plane. As will be shown below, the

closeness of agreement between prediction and measurement is a function of the number of samples available.

In Tables 10 and 11 in the Appendix, the predicted and measured values of $\arctan(\tau/\sigma_n)$ and JRC are compared for 15 individual joint types. Fig. 20 shows examples of these joints and their characteristics are summarized in Table 9 (see Appendix). The comparison of predicted and measured data is divided into three categories: joints with $JRC \leq 8.0$ (tilt testing range), joints with $8.0 < JRC \leq 12.0$ (push testing range), and combined results ($JRC \leq 12.0$).

The following ranges of *mean errors* were found for the 15 varieties of joint: (Note: (+) for overestimate, (-) for underestimate):

- 1) $JRC \leq 8.0$ (*tilt test range*)
 - (a) range of errors in mean predicted $\arctan(\tau/\sigma_n)^0 = -3.0$ to $+3.5^0$.
(mean error for 57 specimens = -0.2^0)
- 2) $8.0 < JRC \leq 12.0$ (*push test range*)
 - (a) range of errors in mean predicted $\arctan(\tau/\sigma_n)^0 = -3.4^0$ to $+4.1^0$.
(mean error for 45 specimens = $+1.3^0$)
- 3) $JRC \leq 12.0$ (*combined*)
 - (a) range of errors in mean predicted $\arctan(\tau/\sigma_n)^0 = -2.4^0$ to $+3.2^0$.
(mean error for 102 specimens = $+0.5^0$)
 - (b) range of errors in mean predicted $JRC = -0.9$ to $+1.4$.
(mean error for 102 specimens = $+0.2$)
 - (c) range of errors in predicted $\arctan(\tau/\sigma_n)^0$ caused by errors in predicting $JRC = -2.2^0$ to $+3.2^0$.
(mean error for 102 specimens = $+0.5^0$)
 - (d) range of errors in predicted ϕ_r implied by the above errors = -1.0^0 to $+0.8^0$.
(mean error for 102 specimens = -0.1^0)

It will be seen from the *combined* results that errors in predicting $\arctan(\tau/\sigma_n)$ for any one rock or joint type may be as high as $\pm 3^0$ (approx.). However, in two cases there was only one push or tilt tested sample from which to "calculate" the mean. If we select only those rock or joint types in which there were more than five samples for *tilt* and/or *push* testing, then the range of errors in predicted $\arctan(\tau/\sigma_n)$ reduces to -1.1^0 to $+1.5^0$ for any one joint or rock type. In the case of granite and aplite in which there were as many as 34 and 22 specimens respectively for tilt and/or push testing, the mean prediction errors were reduced to $+0.3^0$ and -0.4^0 respectively. It would seem that a minimum of ten tests would result in an error in prediction of no more than $\pm 1^0$. (It should not be forgotten that there is inevitable scatter in the shear box tests themselves. This increases the number of samples required to obtain close agreement between mean measured and mean predicted values.)

Range of Peak Shear Strength

In an earlier review article (Barton, 1973, Fig. 17), the results of a large number of direct shear tests reported in the literature were collected, to illustrate the wide spectrum of peak shear strength exhibited by rock joints. Results of both in situ and laboratory tests were included. It was found that

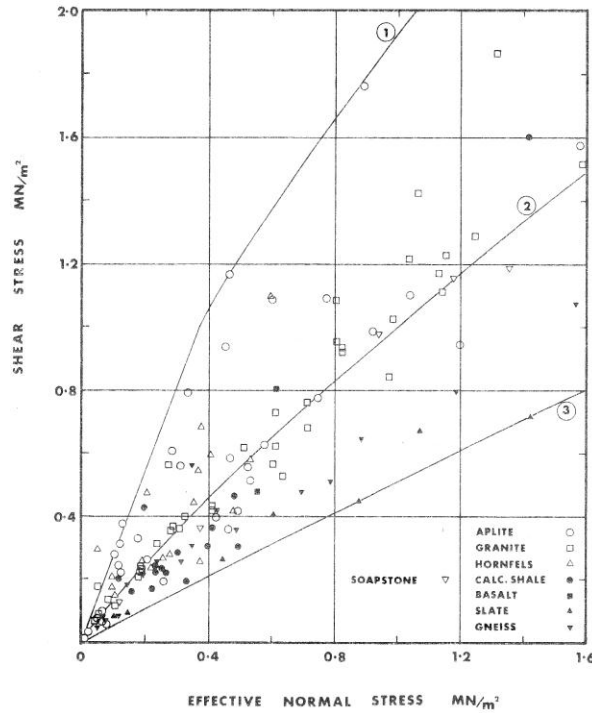


Fig. 14. Range of peak shear strength for 136 joints representing eight different rock types. Curves 1, 2 and 3 are evaluated in the text

Scherfestigkeitsbereich für 136 Klüfte aus acht verschiedenen Felstypen. Die Kurven 1, 2 und 3 sind im Text ausgewertet

Distribution des résistances au cisaillement de 136 joints représentant huit types différents de roche. Les courbes 1, 2 et 3 sont appréciées dans le texte

values of peak arctan (τ/σ_n) ranged from about 28° to 82° for unfilled joints. The greatest concentration of results was in the 40° to 50° range, at least for effective normal stress levels below about 0.6 MN/m^2 .

The present experimental study on 136 joints showed a similar trend to the larger sample referred to above. The results of all the tests are shown in Fig. 14. In this case it was found that values of peak arctan (τ/σ_n) — the *total friction angles* — ranged from 26.6° (smooth, planar cleavage joint in slate) up to 80.3° (rough, undulating bedding joint in nodular hornfels).

This particular joint in slate had a *JRC* value of only 0.4, so even if the *JCS* value had been higher than 50 MN/m^2 , the total friction angle could hardly be much larger than the value of $\phi_r = 26.0^\circ$. In the case of the roughest joint in hornfels the *JRC* value was 17.9, and the *JCS* value 62 MN/m^2 . In this case the *asperity component* ($JRC \cdot \log_{10} JCS/\sigma_n$) was a full 55° , compared with the residual friction angle $\phi_r = 25^\circ$. The measured *peak dilation angle* (maximum value measured at peak strength) was likewise very high: 51.4° . In the case of the slate the peak dilation angle was 0° or at least too small to be detected.

The three curves marked 1, 2 and 3 in Fig. 14 have been derived from the empirical law of friction [Eq. (6)]. Curve 1 has a linear “cut-off” representing the maximum suggested design value of 70° for the total friction angle (see Fig. 1). This seems to be quite a good upper bound in the case of the present 136 joint samples. The remainder of curve 1 has the following equation:

$$(i) \quad \tau = \sigma_n \tan [16.9 \log_{10} (96/\sigma_n) + 29^\circ]$$

Curve 2 represents the mean of all the 136 specimens. The three empirical constants *JRC*, *JCS* and ϕ_r had the following mean values; 8.9, 92 MN/m^2 , and 27.5° .

$$(ii) \quad \tau = \sigma_n \tan [8.9 \log_{10} (92/\sigma_n) + 27.5^\circ]$$

Curve 3 represents the lower bound of the present series of tests, and is evaluated from the following equation:

$$(iii) \quad \tau = \sigma_n \tan [0.5 \log_{10} (50/\sigma_n) + 26^\circ]$$

For those who still prefer to interpret the shear strength of rock joints in terms of Coulombs “constants” c and ϕ , the mean curve (No. 2) could be crudely approximated to $c = 0.04 \text{ MN/m}^2$ and $\phi = 45^\circ$, for the normal stress range 0.05 to 1.0 MN/m^2 . The value $\phi = 45^\circ$ is therefore seen to be a realistic approximation for first order estimates of the peak shear strength of unfilled rock joints, provided the stability problem is not caused by smooth planar joints such as cleavage joints in slate, or strongly weathered joints. One can therefore conclude as a rough rule-of-thumb that a common value of the peak *coefficient of friction* for rock joints is 1.0, but the range may be from 0.5 to 5.0.

Effect of Dilation on Rock Mass Stability

When rock joints are subjected to shearing stress while under normal load the asperities on either side of the joint will tend to slide into contact at a few points along their opposed sloping faces, thereby changing the “at

rest" contact positions. In fact the mating joint walls offer relatively little shear resistance before this initial shear deformation, since dilation (displacement perpendicular to the joint) is virtually absent. However, when the opposed sloping faces of the major asperities make contact the inherent shear characteristics begin to show; the shear strength rises and dilation against the normal load begins. The instant of peak strength is approaching. All this usually occurs before the shear displacement has reached 1% of the length of joint being tested.

In general, a weak rough joint wall (low *JCS*, high *JRC*) will suffer more damage during shear than a strong smooth surface, though neither will dilate strongly. Only those surfaces with high *JCS* and high *JRC* will dilate strongly at the instant of peak strength.

The degree to which a rock joint dilates when sheared is of far reaching consequence in rock mechanics. In fact if it was only possible to choose one parameter to characterise the potential performance of a rock slope, underground excavation, or rock foundation, the peak dilation angle of the critical joints would surely have to rate first in importance.

The *peak dilation angle*, d_n , is the maximum dilation angle which occurs more or less simultaneously with peak shear resistance. In the case of a rock slope the value of the peak dilation angle determines quite simply whether or not one can rely on a shear strength greater than the residual friction angle ϕ_r . If the critical joints are clay filled, or planar, or exhibit signs of earlier shearing then clearly one cannot use anything but ϕ_r in the design. The dilation angle is assumed to be zero for all practical purposes. If on the other hand the joints are non-planar, unfilled and not presheared, and some measures (i. e. bolting) are to be taken to limit future deformation, then the peak dilation angle will give a crude idea of how much larger the available shear strength is than the ϕ_r value. From simple geometrical considerations the total friction angle seems likely to be equal at least to the sum of ϕ_r and d_n :

$$\text{i. e. } \arctan (\tau/\sigma_n) \geq \phi_r + d_n$$

The available shear strength is often likely to be higher than the sum of ϕ_r and d_n since the strength component due to any crushing of the asperities has been ignored.

In the case of an underground opening in rock, potential fall-out of an unstable block may be checked by the dilation of the relevant joints, if the latter are initially mated and non-planar. In this case the confined boundaries will result in a corresponding increase in effective normal stress across the relevant joints, a stabilizing feature usually absent from rock slope stability problems. The increase in effective normal stress will result in a large increase in shear strength if the joints are dilatant rather than planar or clay filled. It is this difference between *dilatant* and *non-dilatant* joints that causes some underground openings to stand permanently unsupported with spans of up to 100 meters, while some small adits cannot even remain permanently unsupported with a span of only 1 meter if the joints are clay filled (Barton, 1976a).

One of the central problems in rock mechanics which has yet to be solved is in fact the reliable modelling of the complicated inter-relationship between shear deformation, dilation, effective normal stress and rock mass stiffness. The most hopeful method of solving this problem seems to be through numerical approximation techniques such as the finite element and finite difference methods. The future success of these techniques undoubtedly

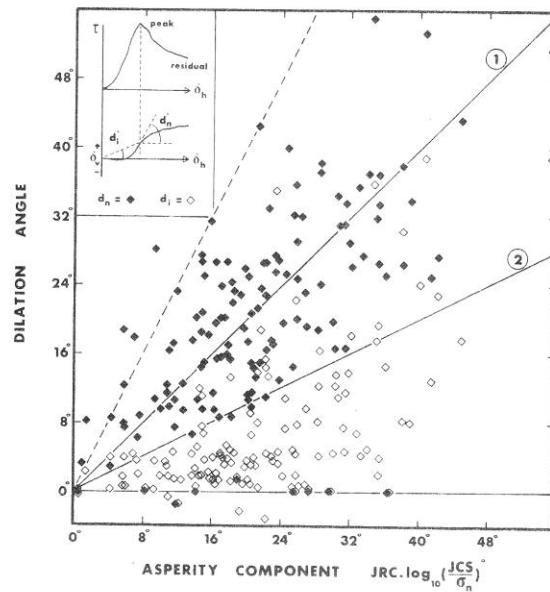


Fig. 15. Distribution of peak and initial dilation angles and their relationship with the asperity component of shear strength

Verteilung von Dilatanzwinkeln am Anfang und bei Höchstscherfestigkeit und deren Verwandtschaft mit dem „Verzahnungsanteil“ der Scherfestigkeit

Distribution des angles initiaux de dilatation et des angles maximums de dilatation et leur rapport à la composante aspérité de la résistance au cisaillement

lies in the incorporation of realistic input data. At present, input data seems to be more or less guessed or extracted from the literature, which is at present limited. Little notice is taken of the stress dependence of almost all the input parameters (i. e. shear strength, stiffness, dilation angle etc.). The scale effect acting on these same parameters is all but ignored.

Relationship Between Asperity Component and Dilation Angle

In this study attempts have been made to rectify the currently poor quality of input data. It has been shown earlier how the empirical constants JRC and JCS can lead to an accurate model of the shear strength. It is now the intention to show how these same empirical constants can be used to estimate the dilation angle for any given joint under a given range of effective normal stress.

The direct shear box used in this study (Engineering Laboratory Equipment ELE 10 cm square) was a modified soil mechanics shear box. (Provision was made for accommodating rough irregular joints by inserting an 8 mm thick low friction "Teflon" (PTFE) spacer to separate the two halves of the box, without disturbing the line of action of the shearing force). The box was provided with sensitive dial gauges (0.002 mm/division) for recording the mean horizontal and vertical deformation during shear. These gauges were read at intervals of 10 seconds. Peak strength was reached after about 5 to 15 minutes shearing. The incremental displacement ratio δ_v/δ_h (δ_v = vertical, perpendicular displacement, δ_h = horizontal, shear displacement) gives a measure of the dilation angle at any given time.

In the present study interest centered on the *peak dilation angle* (d_n^0) and the *initial dilation angle* (d_i^0). These two angles are defined in the inset to Fig. 15. In this figure these two dilation angles are plotted against the asperity component. The latter is equal to the difference between the measured *total friction angle* ($\arctan \tau/\sigma_n$) and the estimated residual friction angle (ϕ_r). Several features may be noted from the distribution of data:

- (i) Both peak and initial dilation angles were occasionally negative or zero. In such cases the joints did not start to dilate significantly until after peak strength was reached, and in fact may have contracted to begin with. When this occurs in spite of a quite high asperity component, it signifies that the joint "failed" when a small steep interlocking projection failed. In such cases there was a negligible *geometrical component* of strength, and a significant *asperity failure component*. Under conventional rock mechanics stress levels such cases are the exception rather than the rule.
- (ii) The majority of peak dilation angles fell between the following limits:

$$0.5 JRC \cdot \log_{10} (JCS/\sigma_n) < d_n < 2 JRC \cdot \log_{10} (JCS/\sigma_n)$$

With the exception of those cases described in (i) above, line 2 in Fig. 15 appears to be a very good lower bound i. e.

$$d_n = 1/2 JRC \cdot \log_{10} (JCS/\sigma_n) \quad (13)$$

- (iii) The middle envelope (line 1) is a close approximation to the mean performance of the 136 joint samples tested here. The overall mean value of d_n^0 for the 136 samples was 20.0° , compared to 21.1° for the *asperity component*. In other words, where asperity damage is slight

(due to relatively high JCS values, or low σ_n values, and/or small JRC values) the following relation gives a first approximation to the *peak dilation angle*.

$$d_n = JRC \cdot \log_{10} (JCS/\sigma_n) \quad (14)$$

- (iv) The mean value of the *initial dilation angle* (d_i) for the 136 specimens was 6.6° , roughly one third that of the *peak dilation angle* (d_n). Thus as a first approximation:

$$d_i = 1/3 JRC \cdot \log_{10} (JCS/\sigma_n) \quad (15)$$

It can be concluded from Eq. (14) that for joints which suffer relatively little damage during shear, the following equation may be used as a first approximation to the peak strength:

$$\tau = \sigma_n \tan (d_n + \phi_r) \quad (16)$$

The Damage Coefficient

A series of direct shear tests on rough model tension fractures that were reported by Barton (1971a), were performed at normal stress levels that resulted in considerably greater asperity damage than that encountered in the present series of tests. In fact JCS/σ_n ranged from about 4.1 to 125 (mean of 29 for 130 artificial fractures). In the present series of shear box tests on natural joints the mean value of JCS/σ_n was 440 (range 15.5 to 5550). The tilt tests and push tests clearly gave much higher values, as can be seen from Fig. 12.

It is significant that Eq. (13) (the lower bound) gave an extremely good fit to the test data obtained from these 130 model fractures. In fact the mean measured *peak dilation angle* for the 130 fractures was 13.15° , while the mean *asperity component* ($JRC \cdot \log_{10} JCS/\sigma_n$) was 26.34° . This close agreement led to the following relationship being suggested for the peak shear strength of rough undulating joints (Barton, 1971a):

$$\tau = \sigma_n \tan (2d_n + 30^\circ) \quad (17)$$

where 30° represented the basic friction angle (ϕ_b) of the unweathered material.

It will have been noted that Eqs. (13) and (17) are relevant to shear tests in which the ratio of JCS/σ_n is low enough for considerable asperity damage to occur, while Eqs. (14) and (16) are relevant to shear tests in which the value of JCS/σ_n is high, such that little damage occurs. In the first case there is a high asperity failure component and a low geometrical component, and in the second case the reverse. It is convenient to define a joint *damage coefficient* as follows:

$$M = \frac{JRC}{d_n} \cdot \log_{10} (JCS/\sigma_n) \quad (18)$$

It follows that a general expression for the peak shear strength will be obtained if Eqs. (16) and (17) are generalized for all states of damage to:

$$\tau = \sigma_n \tan (M d_n + \phi_r) \quad (19)$$

It is of interest to examine the value of M for the eight different rock types studied here, and compare it with the value $M=2.00$ obtained from the high-damage tests on the 130 model tension fractures (Barton, 1971a). Table 5 summarizes the *mean values* for each group of rocks. At the bottom of the table, the results for rough artificial tension fractures in soapstone and in the weak brittle model material are given for comparison with the natural joints. Four samples of calcareous shale exhibited zero dilation. They did not dilate until after peak strength was reached. Only two samples of basalt were available. These results were not included in Table 5.

Table 5. Mean Dilation Angles and Damage Coefficients

Rock type	No. of samples	d_n^0	$\log_{10} \left(\frac{JCS}{\sigma_n} \right)$	JRC	Asperity component $JRC \cdot \log_{10} \left(\frac{JCS}{\sigma_n} \right)$	Damage coefficient (M)
Aplite	36	25.5 ⁰	2.53	9.3	23.5 ⁰	0.92
Granite	38	20.9 ⁰	2.36	8.9	21.0 ⁰	1.00
Hornfels	17	26.5 ⁰	2.72	9.6	26.1 ⁰	0.99
Calcareous shale	11	14.8 ⁰	2.50	8.2	20.5 ⁰	1.39
Slate	7	6.8 ⁰	1.83	2.9	5.3 ⁰	0.78
Gneiss	17	17.3 ⁰	2.26	7.7	17.4 ⁰	1.01
Soapstone	5	16.2 ⁰	1.56	16.6	24.8 ⁰	1.53
Model fractures	130	13.2 ⁰	1.29	21.1	26.3 ⁰	2.00

It will be clear from examination of Table 5 that the estimation of peak dilation angle for a given joint is not a simple matter. The *damage coefficient* is generally higher when JCS/σ_n is low as one would expect, but the value of the joint roughness coefficient (JRC) complicates this picture since smooth joints such as the cleavage joints in slate suffer very little damage, even when the value of JCS/σ_n is low enough to suggest considerable damage. This influence of roughness is of course quite logical, since a steep asperity with a small base area (high JRC) will be sheared off more readily than a gently sloping asperity of large base area (low JRC).

The results given in Table 5 were plotted to dry to establish the main trend of behaviour. A graph of *damage coefficient* (M) versus $JRC/\log_{10} (JCS/\sigma_n)$ established the following approximate relationships as the most reliable for estimating M and d_n .

$$M = \frac{JRC}{12 \cdot \log_{10} (JCS/\sigma_n)} + 0.70 \quad (20)$$

$$d_n^0 = \frac{12 JRC (\log_{10} JCS/\sigma_n)^2}{JRC + 8.4 \log_{10} (JCS/\sigma_n)} \quad (21)$$

The predicted values of d_n and M obtained from these equations are given in Table 6. The agreement is seen to be good, with the notable exception of the calcareous shale. The latter consisted of quite planar joints but with occasional steep ridges and occasional intersecting calcite veins. These features resulted in much higher JRC values than would be expected from

Table 6. Comparison of Predicted and Measured Dilation Angles and Damage Coefficients

Rock type	No. of samples	Measured d_n^0	Predicted d_n^0	Measured M	Predicted M
Aplite	36	25.5 ⁰	23.4 ⁰	0.92	1.01
Granite	38	20.9 ⁰	20.7 ⁰	1.00	1.01
Hornfels	17	26.5 ⁰	26.3 ⁰	0.99	0.99
Calcareous shale	11	14.8 ⁰	21.1 ⁰	1.39	0.97
Slate	7	6.8 ⁰	6.4 ⁰	0.78	0.83
Gneiss	17	17.3 ⁰	17.7 ⁰	1.01	0.98
Soapstone	5	16.2 ⁰	16.7 ⁰	1.53	1.55
Model fractures	130	13.2 ⁰	13.2 ⁰	2.00	2.06

the relatively planar surfaces. However, the measured dilation was unexpectedly low in relation to these unexpectedly high JRC values, due to the amount of asperity damage occurring ($M=1.39$).

While it is easy to understand that the *damage coefficient* M is greater than 1.0 when JCS/σ_n is low and/or when JRC is high, it is rather unexpected to find that M can apparently be less than 1.0. For example the mean value for the seven specimens of cleavage joints in slate was 0.78. The possibility that this is due to experimental errors must be considered, particularly in view of the low mean value of peak dilation angle (6.8⁰) measured on these smooth surfaces. If the minimum value of M is in fact exactly 1.0 as one would expect from "zero-damage" shearing, the discrepancy of 0.22 actually represents only 1.5⁰ mean error. It is quite possible that the experimental errors involved in recording d_n manually from dial gauge readings at intervals of ten seconds will result in errors of larger magnitude than this.

Peak Shear Stiffness and Displacement

The shear displacement δ (peak) required to reach peak shear strength determines the stiffness of joints in shear. This is extremely important input data in finite element analyses of jointed rock, since joints are very deformable in shear compared to the normal direction and compared to the intact rock (Barton, 1972). The peak shear stiffness (K_s) is defined as the peak shear strength (τ) divided by δ (peak). Since we have already developed what appears to be a very reliable method of estimating τ for any given values of JCS , JRC , ϕ_r and σ_n , it only remains to estimate δ (peak) for an estimate of K_s to be obtained.

It can be seen from Table 7 that the mean value of δ (peak) varies from about 0.6 to 1.2 mm for joints in the eight rock types studied. The reason

for the variations is not entirely clear. It does however appear that smoother joints such as the slate, or joints in weathered rock that do not mate very tightly such as the Drammen granite, required greater shear displacement to

Table 7. Variation of Mean δ (Peak) for the Eight Rocks Studied

Rock type	No. of samples	δ (peak) mm	JRC (mean)
Aplite	36	0.89	9.3
Granite	38	1.14	8.9
Hornfels	17	0.78	9.6
Calcareous shale	11	0.59	8.2
Basalt	2	0.69	8.5
Slate	7	1.21	2.9
Gneiss	17	0.86	7.7
Soapstone	5	0.83	16.6

reach peak strength. The overall mean for 136 specimen was 0.93 mm, which represents about 0.95% of the mean joint length (L), which in this case was 9.8 cm.

An earlier study of joint displacement effects by Barton (1971a) indicated that model tension fractures representing prototype joint lengths from 225 cm up to 2925 cm required approximately 1% displacement (i. e. δ (peak)/ $L \approx 0.01$) to reach peak strength throughout this range of simulated joint lengths. The present test results from 10 cm long rock joints appear to fit these observations quite well.

In view of the 1% displacement “rule-of-thumb” the peak shear stiffness $K_s = \tau/\delta$ (peak) is seen to be strongly dependent on scale. In fact a review of laboratory and in situ shear tests (Barton, 1972, Fig. 15) indicated that shear stiffness was indeed inversely proportional to joint length. However, it seems clear that δ (peak) will eventually reduce to less than 1% L as the joint length increases to several metres. (It is suggested in the next section concerning scale effects that the *critical joint length* (L_c) still just sensitive to scale effects on τ and δ (peak) may be controlled by the maximum spacing of cross-joints intersecting the joint of interest. The rock mass will have reduced stiffness and possibly a less marked scale effect if the joint spacing is small).

For most practical purposes the estimate of peak shear stiffness given in Eq. (22) should be adequate as a basis for calculating the appropriate range of input data for a given finite element analysis.

$$K_s = \frac{100}{L} \cdot \sigma_n \tan [JRC \log_{10} (JCS/\sigma_n) + \phi_r] \tag{22}$$

where K_s = peak shear stiffness (MN/m²/m)
 L = joint length (m)

However, if the scale effect does indeed die out when a certain critical length of joint (L_c) is exceeded then the value of L used in Eq. (22) should not exceed L_c .

Scale Effect Investigation

In a recent investigation of scale effects, Pratt et al. (1972) reported a series of unconfined compression tests on samples of quartz diorite, ranging in length from 5 to 275 cm. They found that the compression strength dropped from about 60 or 70 MN/m² for 5 cm long specimens down to about 7 MN/m² for 90 cm long specimens. Further increases in specimen length to 275 cm did not appear to indicate any scale effect beyond a length of about 100 cm. Their results and those of others, suggest that not only σ_c , but potentially also *JCS* must be considered as a scale-dependent variable.

Scale Effect on *JCS*

A subsequent scale effect investigation of the shear strength of joints in quartz diorite (Pratt et al., 1974) showed roughly 40% drop in peak shear strength over a range of surface areas of 60 cm² to 5000 cm². Fig. 16 taken

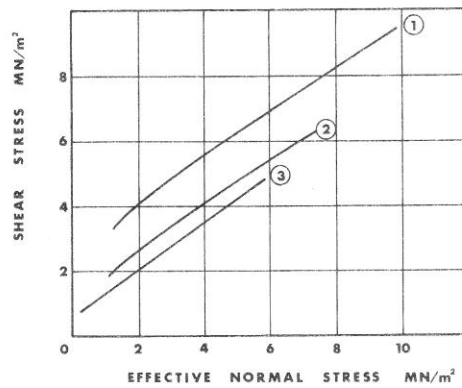


Fig. 16. Results of in situ shear tests on joints in quartz diorite, after Pratt et al. (1974). Envelope (1) represents specimens with an average joint area of approximately 200 cm², (2) an average area of 1500 cm², and (3) an average of 5000 cm².

Resultate von in situ Scherversuchen auf Klufflächen in Quarz-diorite nach Pratt et al. (1974). Die Umhüllungskurven 1, 2, 3 repräsentieren Proben mit Klufflächen von durchschnittlich folgenden Größen: 200 cm², 1500 cm² und 5000 cm².

Résultats d'essais de cisaillement in situ sur joints en quartz diorite, selon Pratt et d'autres (1974). Les enveloppes (1), (2) et (3) représentent des échantillons d'une aire de joint moyenne approximative de respectivement 200 cm², 1500 cm² et 5000 cm².

from Pratt et al. (1974) shows three distinct peak shear strength envelopes for mean joint areas of 200, 1500 and 5000 cm². If square test areas are assumed, these areas represent joint lengths (*L*) of about 14, 39 and 71 cm

respectively. Interpreting their results at an effective normal stress of 1.5 MN/m^2 , peak values of $\arctan(\tau/\sigma_n)$ of approximately 68° , 56° and 48° are obtained for the three scales of test. When the stress level is 3.0 MN/m^2 the corresponding values of $\arctan(\tau/\sigma_n)$ are 58° , 48° and 42° .

A previous interpretation of these results by Barton (1976b) indicated that the three curves shown in Fig. 16 were simulated quite well by the empirical Eq. (2). Values of $JRC=20$ (rough, undulating joints) and $\phi_b=30^\circ$ were assumed, and values of JCS of 54 , 23 and 13 MN/m^2 were back

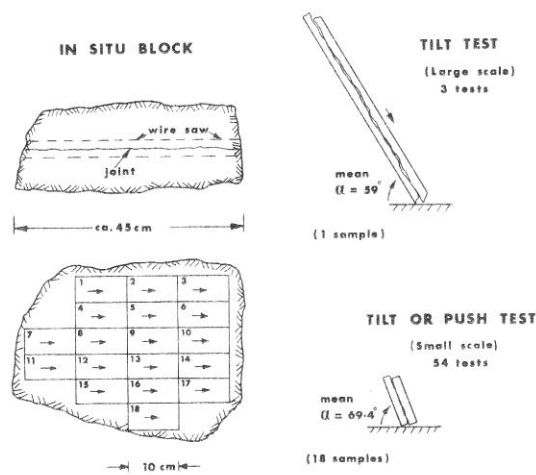


Fig. 17. Tilt tests of large scale and small scale joint samples to investigate the scale effect on JRC . Due to increased roughness ($JRC > 8.0$) 12 of the 18 small samples had to be push tested

Kippversuche mit großen und kleinen Klüftfläche-Proben, um Einfluß der Größe (Maßstabeffekt) auf den JRC -Wert zu untersuchen. Wegen erhöhter Rauigkeit ($JRC > 8,0$) mußten im Versuch 12 von den 18 kleinen Proben geschoben werden

Essais de basculement sur grands et petits échantillons, effectués en vue d'examiner la répercussion de l'effet d'échelle sur le JRC . A cause d'une rugosité accrue ($JRC > 8,0$), il a fallu, à l'essai, pousser 12 des 18 petits échantillons

calculated by fitting the empirical equation to the three experimental curves. The apparent four-fold reduction in JCS values due to this assumed scale effect very roughly corresponded to the reduction in σ_c with increasing sample size recorded by Pratt et al. (1972) in their earlier study of the scale effect on unconfined compression strength. However, the present series of shear tests on joints from the Oslo area has indicated another potential source of scale effect.

Scale Effect on *JRC*

One of the jointed blocks of rock obtained from the Drammen granite (Fig. 9) was of suitable size (ca. 40 cm × 45 cm joint area, 25 cm thick) for a scale effect investigation. There was no equipment available for shearing this large joint area under conventional normal stress levels for comparison with similar tests on smaller samples, so the scale investigation was limited to tilt tests. As it turned out, this experimental limitation was fortuitous.

The block was sawn with a wire saw parallel to both sides of the rough, planar joint. After washing and drying the two resulting 2.3 cm thick mating plates of rock were tilt tested so that sliding occurred down the 45 cm length of the joint (see Fig. 17). Three tilt tests were performed and in each test the tilt angle was 59°. The inclinometer used could not be read to closer than about ±0.5°. The large plate was carefully marked so that it could subsequently be sawn into 18 equal samples measuring 4.9 × 9.8 cm in area with minimum wastage at the edges. The shear direction was marked so that each of the small specimens could be tilt-tested, push-tested, and shear box tested in the same direction as the original tilt test of the 45 cm long joint. The results of this investigation are given in Table 8. The values

Table 8. Results of Tilt, Push and Shear Box Tests on Joints in Drammen Granite ($\phi_r = 29^\circ$)

Sample	α^0 (tilt)	α^0 (push)	$(\tau/\sigma_n)^0$	σ_n (MN/m ²)	<i>JRC</i> (box)	<i>JRC</i> (tilt)	<i>JRC</i> (push)
1	64.0		52.1	0.051	7.2	5.9	
2		69.6	49.5	1.038	10.7		9.9
3	61.8		49.2	0.178	7.6	5.5	
4		70.1	46.0	1.246	9.3		10.6
5	77.0		45.4	0.613	7.7	7.2	
6		76.8	52.1	0.288	9.4		10.7
7		68.9	46.8	1.154	9.6		9.9
8		73.2	46.8	0.713	8.6		10.1
9		68.4	46.0	1.132	9.1		10.0
10		71.9	59.5	0.051	9.5		10.8
11	71.9		43.6	0.715	7.1	6.8	
12	64.2		43.1	0.605	6.6	5.9	
13		67.4	44.1	1.142	8.1		8.9
14		63.4	51.5	0.280	9.1		10.5
15		67.0	48.7	0.824	9.8		10.0
16		75.5	49.6	0.809	10.2		9.8
17	64.2		46.2	0.413	7.5	5.8	
18		73.5	52.7	0.238	9.3		10.8
Mean	67.2 ⁰	70.5 ⁰	48.5	0.638	8.7	8.8 (combined)	

of $\arctan(\tau/\sigma_n)$ obtained from the tilt tests (α^0 tilt) and push tests (α^0 push) are tabulated first, followed by the conventional peak $\arctan(\tau/\sigma_n)$ measured in the shear box under given levels of effective normal stress (σ_n). The mean value of $\log_{10}(JCS/\sigma_n)$ operating in the 18 shear box tests was 2.26.

The 18 small specimens had length/thickness ratios of approximately 4, and the normal stress operating during the tilt tests was estimated by using Eq. (11). However, the tilt tests performed on the large 45 cm long joint had a length/thickness ratio of approximately 20, and this was considered large enough for Eq. (10) (infinite plane solution) to give a more accurate estimate of normal stress than Eq. 11. The JRC value predicted from the three large scale tilt tests was 5.5. [A value of 5.2 would have been obtained using Eq. (11)].

It will be seen from Table 8 that there is a discrepancy between the predicted JRC value of 5.5 obtained from the large scale tilt tests, and the mean value of 8.7 obtained from back analysis of the 18 shear box tests on the small samples. However, the mean value of $JRC=8.8$ estimated from the combined results of tilt and push tests agrees very closely, and allows one to estimate a mean arctan (τ/σ_n) of 48.8° for the 18 small samples, which compares well with the measured mean of 48.5° .

The mean values of $\log_{10} (JCS/\sigma_n)$ operating during the small sample tilt and push tests (5.60), and during the large sample tilt test (5.50) are too close and too large (zero damage) for this to be any source of discrepancy. In fact there seems no possibility that the present scale effect can be due to JCS effects. One must therefore conclude that there was a significant scale effect on JRC , since its value apparently reduced from 8.7 (or 8.8) for the 10 cm long joint samples, to 5.5 for the 45 cm long joint sample from which the small ones were cut. The measured mean arctan (τ/σ_n) of 48.5° obtained from the 10 cm samples is 7.2° larger than the value of 41.3° which is obtained if the large scale tilt test is used to predict peak shear strength under the same mean normal stress ($\log_{10} JCS/\sigma_n=2.26$) as applied in the shear box tests on the small scale samples.

The reasons for the above scale effects on JCS and JRC are related at least qualitatively. It will be remembered that δ (peak) appears to increase roughly in proportion to joint length (L), up to some critical length (L_c). Furthermore, analysis of joint surfaces shows that the longer the base length considered the less steep the asperities (Patton 1966, Rengers 1971, Barton 1971a). It is therefore clear that as the joint length is increased, the inherent stiffness of the surrounding rock will result in joint wall contact being transferred to the *major and less steeply inclined asperities* as peak strength is approached. Thus, on a larger scale there are larger individual contact areas with correspondingly lower JCS values than those of the small steep asperities. The larger contact areas are themselves less steeply inclined in relation to the mean plane of the joint than the small steep asperities, and therefore give correspondingly reduced JRC values.

Allowance for Scale Effects

1. JCS

Miller's (1965) interpretation of compression strength from the Schmidt hammer field index test, provides a small scale (i. e. 5 cm sample length) estimate of JCS and/or σ_c . Pratt et al. (1972), Bieniawski and

Van Heerden (1975) and others have shown that there is a significant scale effect on σ_c up to a sample size of about 100 cm. An approximate ten-fold reduction in strength is documented for coal, and for a rather porous quartz diorite. Denser rocks such as norite, basalt, marble, limestone, and iron ore, though not studied over such a range of sample sizes, show markedly less tendency towards a scale effect. For present purposes it is perhaps wise to use a range of reduction factors, i. e. a maximum two- to three-fold reduction for dense rocks, and a maximum ten-fold reduction for more porous rocks. *JCS* reduction factors of 2.5, 5 and 10 should perhaps be considered as a representative range for the rock types likely to be encountered.

If we consider a *JRC* value of 10, these reduced in situ values of *JCS*/2.5, *JCS*/5 and *JCS*/10 imply reductions of peak arctan (τ/σ_n) of 4° , 7° and 10° respectively. For smoother joints the same reductions in *JCS* would have less effect (see Fig. 1), the reductions being directly proportional to the *JRC* values. It will be shown below that errors in estimating the *JCS* scale reduction factor have only minor influence on the resulting estimate of peak shear strength, since a push, pull or tilt test performed in the field will show a higher apparent *JRC* value if the full scale *JCS* value is underestimated and vice versa.

2. *JRC*

In the case of the quartz diorite joints tested by Pratt et al. (1974), a sample length increase from 14 cm to 71 cm (square joint areas assumed) resulted in the peak value of arctan (τ/σ_n) falling from 68° to 48° for a common normal stress of 1.5 MN/m^2 . This marked scale effect is presumably caused by the combined effect of *JCS* reduction and *JRC* reduction. The observed reduction in σ_c as sample sizes increased (Pratt et al. 1972) suggest that between 12° and 15° of this 20° fall in strength might be attributed to the *JCS* scale reduction factor.

In the case of the Drammen granite joint studied here, the sample length increase from 10 cm to 45 cm resulted in the peak value of arctan (τ/σ_n) falling from a measured mean for 18 samples of 48.5° to a theoretical value of 41.3° . No *JCS* scale reduction factor was involved in this case, and the theoretical 7° reduction in peak strength must be attributed solely to the *JRC* scale reduction factor. The actual reduction of *JRC* from 8.7 to 5.5 is the only experimental result available, and is clearly no basis from which to estimate a range of *JRC* scale reduction factors.

In Situ Push, Pull and Tilt Tests

The problem of estimating scale reduction factors for *JCS* and *JRC* is largely taken care of if *large scale* push, pull or tilt tests are performed in the field. The value of *JRC* backanalysed from such tests will depend on the estimate of ϕ_r , and on the full scale assumed value of *JCS*. (ϕ_r should be independent of scale effects). A typical example is given here to illustrate the effects of incorrect estimation of *JCS*.

Example:

Assumed parameters: $JCS = 100 \text{ MN/m}^2$ (Schmidt rebound tests, Fig. 2)
 $\phi_r = 25^\circ$ (equation 7, Table 1, etc.)
 $\sigma_{n0} = 0.01 \text{ MN/m}^2$ (assumed normal stress acting during in situ push, pull, or tilt tests, i. e. from block thickness $h = 40 \text{ cm}$, $\gamma = 25 \text{ KN/m}^3$)
 $\alpha = 60^\circ$ (tilt angle, or $\arctan \tau/\sigma_{n0}$ in the case of push or pull tests)

Substitution of these values in Eq. (12), gives a single estimate of $JRC = 8.8$. If JCS is assumed to be scale dependent as below, the JRC estimate is found to increase accordingly.

Scale reduction factors:	1. JCS	2. $JCS/2.5$	3. $JCS/5$	4. $JCS/10$
Back calculated JRC :	8.8	9.7	10.6	11.7

The automatic compensation of an underestimated full scale JCS value with a higher back-calculated value of JRC (and vice versa) means that the correct estimation of JCS using a Schmidt hammer, and the correct estimation of an appropriate scale reduction factor is not so critical as might be expected. An idea of the errors involved when extrapolating a push, pull or tilt test to design values of σ_n can be obtained from the following table of $\arctan (\tau/\sigma_n)$ values. Two typical design values of σ_n have been assumed, using the same parameters as in the previous example:

	1. JCS	2. $JCS/2.5$	3. $JCS/5$	4. $JCS/10$
A. $\sigma_n = 0.1 \text{ MN/m}^2$	51.3°	50.3°	49.4°	48.3°
B. $\sigma_n = 1.0 \text{ MN/m}^2$	42.5°	40.6°	38.8°	36.7°

It can be seen from the above values of $\arctan (\tau/\sigma_n)$ that a hypothetical in situ push, pull or tilt test will give an overestimate of peak strength by some 3° to 6° if no allowance is made for a reduced JCS when in fact there should be a tenfold reduction in strength. In practice such a gross error is unlikely, and it seems realistic to expect the error from this source to be nearer 1° or 2° for the above range of normal stress.

It can be seen from the above values of $\arctan (\tau/\sigma_n)$ that the errors in estimation are reduced if the extrapolation from in situ push, pull or tilt tests to design normal stresses is limited. In the above example, an extrapolation of JRC over one order of stress magnitude (0.01 to 0.1 MN/m^2) resulted in approximately half the predicted errors of a two orders of magnitude extrapolation. (When no scale effect is involved JRC can be extrapolated reliably over at least five orders of stress magnitude, as shown in Fig. 12).

The problems of scale effect will therefore be minimised by conducting push, pull, or tilt tests on large blocks, preferably the largest that it is pos-

sible to handle economically. It will be appreciated that the object of these prediction methods is to reduce the time and cost of shear strength investigations, while at the same time increasing reliability through a large number of tests. It will not generally be practical to use a wire saw, or line drilling to free the back of blocks, though sometimes such measures might be unavoidable when installing hydraulic jacking equipment, as in the case of very large blocks. However, this amount of effort and expense is negligible in comparison with that normally involved when preparing for large-scale in situ shear tests under *design stress levels*. Normal and shear loads of tens or even hundreds of tons have usually to be applied on these large joint areas.

Joint Spacing Controlling the Scale Effect

From present economic considerations, the inherent joint spacing of a given rock mass will more or less determine the size of block that can be economically pushed, pulled or tilt-tested. However, the natural block size may be something more significant than simply a practical test-size limit. Bearing in mind the effect that joints have in reducing the stiffness of a rock mass, it may be that the scale effect will die out earlier if the joint spacing and block size is small. The rock mass may not be stiff enough for the really large scale asperities to be mobilized as the *only* rock wall contact areas, as might be the case if the rock mass was very massive with widely spaced joints.

For example, if the 45 cm long joint in Drammen granite (Fig. 17) had been divided into 10 cm lengths, representing in situ cross joints at 10 cm spacing, it is probable that the scale effect on *JRC* would have been less marked, and maybe even non-existent. The individual blocks would have moved somewhat independently during shear, thereby maintaining closer contact across the smaller, steeper asperities. When on the other hand, the 45 cm joint is not intersected by cross joints, the inherent stiffness of the intact rock allows larger voids to open up, and peak strength is not reached until after a larger displacement when the major, flatter asperities are in contact. This concept is illustrated in Fig. 18.

One can tentatively conclude, and certainly must hope, that push pull or tilt tests performed on naturally occurring in situ blocks may be on a large enough scale to minimize *JRC* scale effects. If the spacing of cross-joints is 50 cm, then joints of 50 cm length should ideally be pushed, pulled or tilt-tested. If the spacing of cross-joints is 200 cm correspondingly larger blocks should be tested if physically or economically possible. As a first approximation these block lengths will hopefully represent the *critical joint length* (L_c) still just sensitive to scale effects on τ and δ (peak).

A complicating factor might be present if cross-joints were rough, non-planar, and mated, since then the rock mass would remain quite stiff due to the high peak shear stiffness of these joints, especially when under confined conditions within a rock mass. However, as a general observation it is probably true to say that closer spaced joints are often smoother and

more planar than widely spaced joints. Thus the proposed concept whereby the natural block size is related to the *critical joint length* (L_c) may be acceptable.

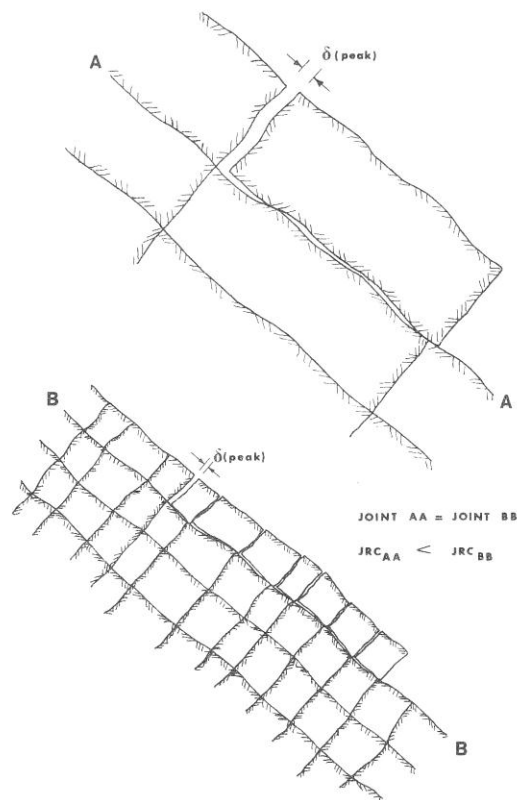


Fig. 18. Cross-joints reduce the stiffness of a rock mass, and probably reduce the scale effect on τ , $\delta(\text{peak})$, K_s and d_n . The magnitude of $\delta(\text{peak})$ is exaggerated for clarity
 Querklüfte reduzieren die Steifigkeit einer Felsmasse, und wahrscheinlich reduziert sich dabei auch der Maßstabeffekt auf τ , $\delta(\text{peak})$, K_s und d_n . Die Größe von $\delta(\text{peak})$ ist klarheitshalber übertrieben gezeichnet

Les joints entrecroisés réduisent la rigidité d'une roche, et réduisent probablement l'effet d'échelle sur τ , $\delta(\text{peak})$, K_s et d_n . La valeur de $\delta(\text{peak})$ a été exagérée pour plus de clarté

Critical State Concept

The overall accuracy with which the empirical law of friction:

$$\tau = \sigma_n \tan \left[JRC \log_{10} \left(\frac{JCS}{\sigma_n} \right) + \phi_r \right] \quad (23)$$

predicts peak shear strength is surprising. It will be remembered that the 57 joints with $JRC \leq 8.0$ were tilt tested under effective normal stress levels so low that the ratio of JCS/σ_n ranged from 10^5 to 10^7 . Yet the same test results could be extrapolated to stress levels more than four orders of mag-

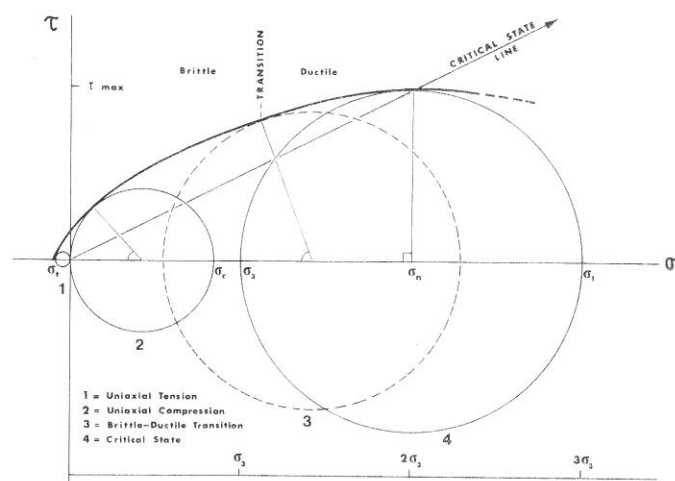


Fig. 19. Typical envelope of failure for intact rock. At the critical state the confined compression strength $\sigma_1 - \sigma_3 (= JCS)$ is of equal magnitude to the mobilized effective normal stress (i. e. $JCS/\sigma_n = 1$)

Typische Hüllkurve für Bruchzustand gesunder Felsen. Im Grenzfall ist die (dreiaxige) Bruchfestigkeit $\sigma_1 - \sigma_3 (= JCS)$ von derselben Größe wie der wirksamen Normalspannung, d. h. $JCS/\sigma_n = 1$

Enveloppe typique d'une rupture de roche saine. A l'état limite, la résistance selon trois axes $\sigma_1 - \sigma_3 (= JCS)$ est du même ordre de grandeur que la tension normale en jeu (c.-à-d. $JCS/\sigma_n = 1$)

nitude higher to give a mean estimation error of $\arctan(\tau/\sigma_n)$ of only 0.2° for the 57 joint samples, when compared with the conventional shear box tests performed on the same samples.

The recent discovery of what is possibly a universal *critical state* for rock (Barton 1976b) may give a clue to the above performance. It appears from a wide survey of high pressure triaxial data that the Mohr envelopes

representing the peak shear strength of *intact* rocks eventually reach a point of zero gradient on crossing a certain *critical state line*. This line has a gradient of $1/2$ (i. e. $\tau/\sigma_n = 1/2$) as shown in Fig. 19.

The ultimate shear strength represented by the top point of a Mohr envelope is associated with a *critical effective confining pressure* for each rock. The major and minor principal effective stresses (σ_1) and (σ_3) associated with failure at the critical state are in the ratio of 3 to 1 (i. e. $\sigma_1 = 3\sigma_3$).

The significant link between this *fracture* behaviour and the present *frictional* behaviour is the following. The effective normal stress (σ_n) mobilized on the orthogonal conjugate failure surfaces at the critical state is found to be equal to the confined strength of the rock ($\sigma_1 - \sigma_3$) (i. e. $\sigma_n = \sigma_1 - \sigma_3$). This happens to be the limiting value of the dimensionless ratio $(\sigma_1 - \sigma_3)/\sigma_n$ used in formulating an empirical law of friction for high pressure tests on fractured rock (Barton 1976b).

$$\tau = \sigma_n \tan \left[JRC \log_{10} \left(\frac{\sigma_1 - \sigma_3}{\sigma_n} \right) + \phi_b \right] \quad (24)$$

Under very high normal stress levels (i. e. $\sigma_n \geq \sigma_c$) the *JCS* value increases to the confined compression strength ($\sigma_1 - \sigma_3$) of the rock. The increase in *JCS* is thought to be caused by the increasing *contact area* and consequently improved confining effect as the normal stress is increased.

It will be remembered from earlier in this paper that the real contact area over which asperities are visibly damaged or scratched is a very small fraction of the apparent total area used for calculating the effective normal stress σ_n . In fact it appears from examination of the present 136 joint samples, and earlier experiences with model tension fractures that as a rough rule-of-thumb, the *total visible contact area* A_1 appears to be related to the sample area A_0 in the ratio σ_n/JCS (i. e. $A_0/A_1 \approx JCS/\sigma_n$). It should be emphasised that the 136 samples were taken only to peak strength, so the increased damage that results from large displacements was not a complicating factor here. In the present study JCS/σ_n ranged from 15.5 to 5550. There was a correspondingly large range of contact areas.

We therefore have a plausible explanation for the phenomenon of peak shear strength. Before the onset of shearing a joint that is mated may have a relatively large area of asperities in contact. However, once shearing commences under a given effective normal stress, the contact area begins to reduce. Possibly the instant of peak strength is reached when the contact area is sufficiently small for the relevant asperities to have reached their limiting state (i. e. $\sigma_n \text{ real} = JCS$). This would be the limit of their shear resistance.

Since *JCS* eventually increases with A_1 due to an improved confining effect as A_1 approaches A_0 , the normal stress level required to mobilize the limiting state (in this case the *critical state*) over the whole joint area A_0 can be markedly higher than the unconfined compression strength σ_c . For example, in the case of Westerly granite it can be shown that $JCS_{\text{crit.}} = 11 \sigma_c$, while for Solenhofen limestone $JCS_{\text{crit.}} = 2 \sigma_c$. (See Fig. 14, Barton 1976b).

Design Implications and Conclusions

1. The residual friction angle (ϕ_r) of a rock joint represents the minimum shear strength. Joints that are smooth and planar, or those that exhibit signs of earlier movement cannot be relied upon to have any asperity component of shear strength and in such cases design (i. e. rock slope design) would have to be based on this minimum shear strength (ϕ_r).
2. A method has been developed for estimating ϕ_r . This is based on two simple index tests: firstly the ratio r/R between the Schmidt rebound on the joint wall and on the unweathered rock, and secondly on *residual tilt tests* which give a measure of the basic friction angle ϕ_b for smooth unweathered rock surfaces. ($\phi_r \leq \phi_b$). Tests on eight different rock types have indicated that ϕ_r can be estimated to within $\pm 1^\circ$, based on these index tests alone. There is unlikely to be any scale effect on the Schmidt rebound ratio r/R (since both values would be equally affected), nor is there likely to be a scale effect on the *residual tilt test* for determining ϕ_b . Thus the value of ϕ_r obtained from Eq. (7) should be independent of scale.
3. If joints are non-planar, not pre-sheared, and some measures (i. e. bolting) are to be taken to limit future deformations, then the peak shear strength represented by the *total friction angle* ($\arctan \tau/\sigma_n$) can generally be relied upon for design purposes. Methods are described for estimating $\arctan \tau/\sigma_n$ based on Schmidt hammer tests (for estimating *JCS*) and based on tilt, push or pull tests (for estimating *JRC*). Present results which are based on 136 joint samples, suggest that the mean value of $\arctan \tau/\sigma_n$ can be estimated to within $\pm 1^\circ$ if a minimum of ten samples are available for index testing. However these estimates take no account of the scale effect on *JCS* and *JRC*.
4. The scale effect on *JCS* and *JRC* is best allowed for in two stages. Firstly a reduced value of in situ joint wall compressive strength should be estimated (i. e. $JCS/2.5$ for dense rocks). In situ push, pull or tilt tests that are back analysed using the reduced in situ estimate of *JCS* should automatically give a full scale value of *JRC* (provided large blocks are tested). Furthermore the *JRC* value obtained will automatically compensate for inevitable errors in the *JCS* estimates. Errors from these sources appear unlikely to exceed $\pm 2^\circ$.
5. The scale dependent values of *JCS* and *JRC* result in scale effects on the *initial* and *peak* dilation angles (d_i) and (d_n), on the shear stiffness K_s and of course on the total friction angle (peak $\arctan \tau/\sigma_n$). Rock mechanics design that is based on the finite element method, for example the prediction of displacements caused by foundation loads, tunnel excavation, or slope excavation, must clearly incorporate the full-scale values of *JCS* and *JRC* so that the relevant values of $\arctan (\tau/\sigma_n)$, d_i , d_n and K_s are obtained. All these parameters are affected by the level of effective normal stress, in addition to their scale dependency.
6. The advent of computer-based design methods such as the finite element technique has resulted in a growing trend to conduct sensitivity analyses.

Input parameters are varied independently to investigate the effect of incorrect assumptions on the end result. In view of the questionable nature of much of the input data this practice has obvious merits. However, the present studies demonstrating the mutual dependence of τ , d_t , d_n , K_s and JRC on the assumed value of JCS , suggest that

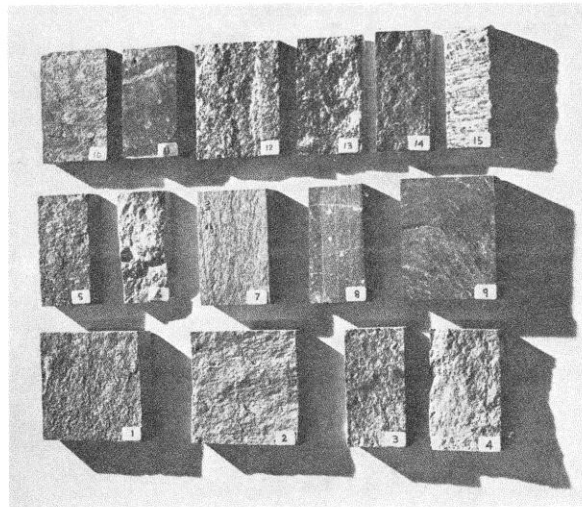


Fig. 20. Photograph illustrating the range of joint surfaces and rock types tested. See Table 9 for descriptions

Das Bild zeigt den Bereich von Kluftflächen und Gesteinsarten, die untersucht wurden. Siehe Tafel 9 für Beschreibungen

Photographie illustrant l'étendue des surfaces des joints ainsi que les types de roche soumis aux essais. Pour description, voir Tableau 9

independent variation of single parameters may be introducing incompatible elements in the numerical model. For example, it is physically incorrect to vary the assumed dilation angle without in some way varying the shear strength and stiffness, unless the residual friction angle (ϕ_r) can be suitably adjusted. This problem emphasises the value of realistic physical modelling in which the parameters are automatically compatible due to their inherent physical equilibrium.

7. In view of the findings described in this paper it is suggested that sensitivity analyses are performed on JRC and JCS rather than on their dependent variables τ , d_t , d_n and K_s . Reducing JRC and/or JCS is equivalent to investigating the effect on design of an unseen joint

having reduced roughness and/or increased weathering of the joint walls. This would be an extremely relevant sensitivity analysis, since with the more sophisticated prediction methods now developed, it is the unseen geological features that have more effect on stability than prediction errors of a few percent.

Acknowledgements

The research described in this report has been sponsored by the Royal Norwegian Council for Scientific and Industrial Research (NTNF). This support is gratefully acknowledged. The second author was a Research Fellow at NGI during the course of this shear strength investigation. His financial support is also much appreciated. Kaare Høeg and Johnny Lunde kindly read the first draft and made valuable suggestions for improvement.

Appendix

Fifteen different types of joint were tested in this shear strength investigation. Eight different rock types were represented. Examples of the 15 joint types are shown in Fig. 20. A brief description of the rock and

Appendix
Table 9. Description of the 15 Joint Types Illustrated in Fig. 20

Joints types	Rock and joint type	Number of samples	JRC (mean)
1	Aplite: smooth, planar tectonic joints (fresh)	13	6.4
2	Aplite: rough, undulating relief joints (fresh)	10	10.7
3	Granite: rough, planar tectonic joints (weathered)	11	9.4
4	Aplite: rough, planar tectonic joints (fresh)	13	11.2
5	Granite: rough, planar tectonic joints (weathered)	27	8.8
6	Hornfels: rough, undulating bedding joints (calcite)	5	13.8
7	Hornfels: smooth, planar tectonic joints (fresh)	12	7.9
8	Calcareous shale: smooth, planar cleavage joints (calcite)	15	8.6
9	Basalt: smooth, planar tectonic joint (fresh)	1	4.2
10	Basalt: rough, undulating tectonic joint (weathered)	1	12.9
11	Slate: smooth, planar cleavage joints (iron staining)	7	2.9
12	Gneiss (muscovite): rough, planar foliation joints (iron staining)	3	5.5
13	Gneiss (muscovite): rough, planar foliation joints (fresh)	7	9.5
14	Gneiss (biotite): smooth, undulating foliation joints (fresh)	7	7.0
15	Soapstone: irregular, undulating artificial tension fractures	5	16.3

surface characteristics (including mean *JRC*) is given in Table 9. The same joint type numbers (1 to 15) are used in each case.

Appendix
Table 10. Peak Strength Prediction Based on Individual Results of Tilt and Push Tests

Joint type	Strength prediction based on Tilt Tests ($JRC \leq 8.0$)				Strength prediction based on Push Tests ($8.0 < JRC \leq 12.0$)			
	1 ⁽¹⁾ Number	2 ⁽²⁾ $\tan^{-1}(\tau/\sigma_n)^0$ (measured)	3 ⁽³⁾ $\tan^{-1}(\tau/\sigma_n)^0$ (predicted)	4 ⁽⁴⁾ Error	5 ⁽¹⁾ Number	6 ⁽²⁾ $\tan^{-1}(\tau/\sigma_n)^0$ (measured)	7 ⁽³⁾ $\tan^{-1}(\tau/\sigma_n)^0$ (predicted)	8 ⁽⁴⁾ Error
1	9	43.1 ⁰	42.0 ⁰	-1.1 ⁰	0	—	—	—
2	2	47.4 ⁰	44.4 ⁰	-3.0 ⁰	5	54.1 ⁰	56.7 ⁰	+2.6 ⁰
3	4	42.9 ⁰	46.4 ⁰	+3.5 ⁰	4	50.5 ⁰	50.3 ⁰	-0.2 ⁰
4	3	43.7 ⁰	43.2 ⁰	+1.5 ⁰	3	55.1 ⁰	51.7 ⁰	-3.4 ⁰
5	8	46.8 ⁰	44.1 ⁰	-2.7 ⁰	18	50.6 ⁰	52.5 ⁰	+1.9 ⁰
6	0	—	—	—	1	55.4 ⁰	53.4 ⁰	-2.0 ⁰
7	6	44.1 ⁰	45.7 ⁰	+1.6 ⁰	4	57.7 ⁰	59.0 ⁰	+1.3 ⁰
8	7	37.3 ⁰	36.6 ⁰	-0.7 ⁰	5	44.6 ⁰	46.5 ⁰	+1.9 ⁰
9	1	41.0 ⁰	38.6 ⁰	-2.4 ⁰	0	—	—	—
10	0	—	—	—	0	—	—	—
11	7	31.5 ⁰	32.7 ⁰	+1.2 ⁰	0	—	—	—
12	3	36.7 ⁰	36.9 ⁰	+0.2 ⁰	0	—	—	—
13	2	35.3 ⁰	37.2 ⁰	+1.9 ⁰	3	47.4 ⁰	51.5 ⁰	+4.1 ⁰
14	5	36.8 ⁰	37.5 ⁰	+0.7 ⁰	2	44.9 ⁰	44.9 ⁰	0 ⁰
15	0	—	—	—	0	—	—	—
Mean	57	40.5 ⁰	40.3 ⁰	-0.2 ⁰	45	50.9 ⁰	52.2 ⁰	+1.3 ⁰

(1) Number of samples of suitable roughness for tilt or push testing.
 (2) Mean measured value of peak arctan $(\tau/\sigma_n)^0$ from shear box tests on the relevant tilt- or push-test samples.
 (3) Mean predicted value of peak arctan $(\tau/\sigma_n)^0$ based on JRC back-analysed from tilt or push tests on same samples as (2).
 (4) Prediction error in degrees: (+) for overestimate, (-) for underestimate.

Appendix
Table 11. Errors in Peak and Residual Strength Prediction, Based on the Combined Results of Tilt and Push Tests

Joint type	Strength prediction based on Tilt and Push Tests ($JRC \leq 12$)				Predicted JRC based on Tilt and Push Tests ($JRC \leq 12$)			Strength prediction errors due to errors in predicting JRC and ϕ_r		
	1 ⁽¹⁾ Number	2 ⁽²⁾ $\tan^{-1}(\tau/\sigma_n)^0$ (measured)	3 ⁽³⁾ $\tan^{-1}(\tau/\sigma_n)^0$ (predicted)	4 ⁽⁴⁾ Error	5 ⁽⁵⁾ JRC (meas.)	6 ⁽⁶⁾ JRC (pred.)	7 ⁽⁷⁾ Error	8 ⁽⁸⁾ JRC error	9 ⁽⁹⁾ ϕ_r error	10 ϕ_r (assumed) [Eq. (7)]
1	9	43.1 ⁰	42.0 ⁰	-1.1 ⁰	5.1	4.4	-0.7	-1.9 ⁰	+0.8 ⁰	31 ⁰
2	7	52.2 ⁰	53.2 ⁰	+1.0 ⁰	8.5	9.1	+0.6	+1.8 ⁰	-0.8 ⁰	29 ⁰
3	8	46.7 ⁰	46.4 ⁰	-0.3 ⁰	7.8	7.6	-0.2	-0.5 ⁰	+0.2 ⁰	29 ⁰
4	6	49.4 ⁰	48.4 ⁰	-1.0 ⁰	7.8	7.6	-0.2	-0.5 ⁰	-0.5 ⁰	29 ⁰
5	26	49.4 ⁰	49.9 ⁰	+0.5 ⁰	8.6	8.8	+0.2	+0.3 ⁰	0 ⁰	29 ⁰
6	1	55.4 ⁰	53.4 ⁰	-2.0 ⁰	10.9	10.2	-0.7	-2.0 ⁰	0 ⁰	25 ⁰
7	10	49.5 ⁰	51.0 ⁰	+1.5 ⁰	6.9	7.8	+0.9	+2.5 ⁰	-1.0 ⁰	30 ⁰
8	12	40.3 ⁰	40.7 ⁰	+0.4 ⁰	7.0	7.2	+0.2	+0.5 ⁰	-0.1 ⁰	23 ⁰
9	1	41.0 ⁰	38.6 ⁰	-2.4 ⁰	4.2	3.3	-0.9	-2.2 ⁰	-0.2 ⁰	30 ⁰
10	0	—	—	—	—	—	—	—	—	25 ⁰
11	7	31.5 ⁰	32.7 ⁰	+1.2 ⁰	2.9	3.5	+0.6	+1.2 ⁰	0 ⁰	26 ⁰ (meas.)
12	3	36.7 ⁰	36.9 ⁰	+0.2 ⁰	5.5	5.5	0	0 ⁰	+0.2 ⁰	24 ⁰
13	5	42.6 ⁰	43.8 ⁰	+1.2 ⁰	7.8	9.2	+1.4	+3.2 ⁰	0 ⁰	25 ⁰
14	7	39.1 ⁰	39.6 ⁰	+0.5 ⁰	7.0	7.0	0	0 ⁰	+0.5 ⁰	23 ⁰
15	0	—	—	—	—	—	—	—	—	19 ⁰
Mean	102	45.1 ⁰	45.6 ⁰	+0.5 ⁰	7.2	7.4	+0.2	+0.5 ⁰	-0.1 ⁰	27.6 ⁰

- (1) Number of samples of suitable roughness for tilt and push testing.
(2) Mean measured value of peak arctan $(\tau/\sigma_n)^0$ from shear box tests on the relevant tilt- and push-test samples.
(3) Mean predicted value of peak arctan $(\tau/\sigma_n)^0$ based on JRC back-analysed from tilt and push tests on same samples as (2).
(4) Prediction error: (+) for overestimate, (-) for underestimate.
(5) Mean measured JRC obtained from back-analysis of shear box tests on relevant tilt- or push-test samples.
(6) Mean predicted JRC obtained from back-analysis of tilt and push tests on same samples as (5).
(7) Prediction error: (+) for overestimate, (-) for underestimate.
(8) Error in predicting peak arctan $(\tau/\sigma_n)^0$ caused by error in JRC value (column 7): (+) for overestimate, (-) for underestimate.
(9) Implied error in ϕ_r estimate as calculated from Eq. (7). (Column 4 — Column 8): (+) for overestimate, (-) for underestimate.

Tables 10 and 11 show the individual prediction errors when comparing measured arctan (τ/σ_n) with the value predicted from the tilt and push tests. The comparison of predicted and measured arctan (τ/σ_n) is divided into three parts:

Table 10. $JRC \leq 8.0$ (tilt-test range)
 $8.0 < JRC \leq 12.0$ (push-test range)

Table 11. $JRC \leq 12.0$ (combined tilt and push tests)

Columns 5, 6 and 7 of Table 11 show the individual errors in predicting JRC from the combined results of tilt and push tests. Column 8 shows the error this causes in predicting arctan (τ/σ_n)⁰, and column 9 shows the implied resultant error in the ϕ_r estimate. The values of ϕ_r assumed in the strength prediction exercise were obtained from *residual tilt tests* and Schmidt hammer tests [using Eq. (7)]. These were corrected to the nearest whole number (Column 10, Table 11). In view of the small range of errors (+0.8° to -1.0°) for the 15 joint types, the decimal points could perhaps have been retained with advantage. Note that joint type 11 (slate) was taken all the way to *residual strength* in the shear box tests. The value 26° given in column 10 of Table 11 is the measured value. The slate was so fissile that no samples remained after sawing that were large enough for Schmidt rebound (R) tests. In this instance ϕ_r could not be estimated from Eq. (7).

References

- Barton, N.: A relationship between joint roughness and joint shear strength. Proc. Int. Symp. on Rock Mech. Rock Fracture. Nancy. Paper I-8 (1971a).
- Barton, N.: Estimation of in situ shear strength from back analysis of failed rock slopes. Proc. Int. Symp. on Rock Mech. Rock Fracture. Nancy. Paper II-27 (1971b).
- Barton, N.: A model study of rock joint deformation. Int. J. Rock. Mech. Min. Sci. 9, pp. 579—602 (1972).
- Barton, N.: Review of a new shear strength criterion for rock joints. Engineering Geology. Elsevier, 7, pp. 287—332 (1973).
- Barton, N.: Unsupported underground openings. Rock Mechanics Discussion Meeting. BeFo, Stockholm, February 1976 (1976a).
- Barton, N.: The shear strength of rock and rock joints. Int. J. Rock Mech. Min. Sci. and Geomech. Abstr. 13, pp. 255—279 (1976b).
- Bienawski, Z. T., and W. L. Van Heerden: The significance of in situ tests on large rock specimens. Int. J. Rock Mech. Min. Sci. and Geomech. Abstr. 12, pp. 101—113 (1975).
- Broch, E.: The influence of water on some rock properties. Proc. 3rd Cong. of Int. Soc. Rock Mech. Denver, Colo., Vol. II, A, pp. 33—38 (1974).
- Broch, E., and J. A. Franklin: The point-load strength test. Int. J. Rock Mech. Min. Sci. 9, pp. 669—697 (1972).
- Byerlee, J. D.: Frictional characteristics of granite under high confining pressure. J. Geophys. Res. 72, pp. 3639—3648 (1967).

- Coulson, J. H.: Shear strength of flat surfaces in rock. Proc. 13th Symp. on Rock Mech. Urbana, Ill., 1971. (E. J. Cording, Ed.), pp. 77—105 (1972).
- Hutchinson, J. N.: Field and laboratory studies of a fall in Upper Chalk cliffs at Joss Bay, Isle of Thanet. In: Stress-strain behaviour of soils (R. H. G. Parry, Ed.). Proc. Roscoe Mem. Symp. Cambridge Univ., 1971, G. T. Foulis, Henley-on-Thames, pp. 692—706 (1972).
- Jaeger, J. C.: The frictional properties of joints in rock. *Geofis. Pura Appl. Milano*, 43, pp. 148—158 (1959).
- Jaeger, J. C.: Friction of rocks and stability of rock slopes. *Geotechnique* 21, pp. 97—134 (1971).
- Krsmanović, D.: Initial and residual shear strength of hard rocks. *Geotechnique* 17, pp. 145—160 (1967).
- Krsmanović, D., and Z. Langof: Large scale laboratory tests of the shear strength of rocky material. *Rock Mech. Eng. Geol. Suppl.* 1, pp. 20—30 (1964).
- Lane, K. S., and W. J. Heck: Triaxial testing for strength of rock joints. In: Proc. Symp. Rock. Mech. 6th, Rolla, Miss., 1964, (E. M. Spokes and C. R. Christiansen, Eds.), pp. 98—108 (1964).
- Martin, G. R., and P. J. Millar: Joint strength characteristics of a weathered rock. Proc. of 3rd Cong. of ISRM. Denver. *Advances in Rock Mechanics*. Vol. II. A., pp. 263—270 (1974).
- Miller, R. P.: Engineering classification and index properties for intact rock. Ph. D. Thesis. Univ. Ill., pp. 1—332 (1965).
- Patton, F. D.: Multiple modes of shear failure in rock and related materials. Ph. D. Thesis. University of Ill. pp. 1—282 (1966).
- Pratt, H. R., A. D. Black, W. S. Brown, and W. F. Brace: The effect of specimen size on the mechanical properties of unjointed diorite. *Int. J. Rock Mech. Min. Sci.* 9, pp. 513—529 (1972).
- Pratt, H. R., A. D. Black, and W. F. Brace: Friction and deformation of jointed quartz diorite. Proc. 3rd Cong. of Int. Soc. Rock. Mech. Denver, Colo., Vol. II. A, pp. 306—310 (1974).
- Rengers, N.: Unebenheit und der Reibungswiderstand von Gesteinstrennflächen. Diss. Tech. Hochschule Fridericiana, Karlsruhe, Ins. Bodenmech. Felsmech. Veröff. 47, pp. 1—129 (1971).
- Richards, L. R.: The shear strength of joints in weathered rock. Ph. D. Thesis. Univ. of London, Imperial College, pp. 1—427 (1975).
- Ripley, C. F., and K. L. Lee: Sliding friction tests on sedimentary rock specimens. Trans. 7th Int. Congr. Large Dams. Rome 1961. Vol. 4, pp. 657—671 (1962).
- Wallace, G. B., E. J. Slebir, and F. A. Anderson: Foundation testing for Auburn Dam. Proc. 11th Symp. on Rock Mech. Berkeley, Calif., 1969. (W. H. Somerton, Ed.), pp. 461—498 (1970).

Addresses of the authors: Dr. Nick Barton, Norwegian Geotechnical Institute, P. O. Box 40, Taasen, N-Oslo 8, Norway; Dr. Vishnu Choubey, Department of Geology, Regional Engineering College, Kurukshetra, India.